PATIENT SPECIFIC LUMPED PARAMETER MODELING OF PENILE ERECTION MECHANISM RELYING ON REDUCED PENILE DOPPLER ULTRASOUND DATA

by

Canberk Yıldırım

B.S., Mechanical Engineering, Yildiz Technical University, 2016

Submitted to the Institute for Graduate Studies in
Science and Engineering in partial fulfillment of
the requirements for the degree of
Master of Science

Graduate Program in Mechanical Engineering

Boğaziçi University

2020

ACKNOWLEDGEMENTS

First of all, I would like to express my deepest gratitude and sincere thanks to my advisor, Prof. Hakan Ertürk and my co-advisor Prof. Kerem Pekkan, who have always contributed to my academic development and scientific vision with their academic support, motivation and kind patience. I am also so grateful to Prof. Ege Can Şerefoğlu for teaching me the all that I know about the human anatomy in an enjoyable way. Without their mentorship, encouragement and motivation, this study would never come to end. Besides, I would like to thank Dr. Sinan Deniz for conducting the required clinical studies for this thesis.

I could not have completed this study without my family's endless support. They have always behind me, stood by me, and helped me to overcome the difficulties. I feel so lucky to have such a great family and I would like to thank my mother Betül, my father Serdar and my sister Eda.

I also would like to thank each of the TESLAB members for their valuable friendship. In addition, special thanks goes to Çayan for being my brother-in-arms during that bumpy road. This study became more enjoyable with their help and precious contribution during three years. In addition, I would like to thank my highschool friends, who have encouraged and supported me during my whole master study.

Once and for all, I would like to dedicate this thesis to my dear love Zeynep, for her existence, deep understanding, indefinite patience and wholehearted support during my master study.

ABSTRACT

PATIENT SPECIFIC LUMPED PARAMETER MODELING OF PENILE ERECTION MECHANISM RELYING ON REDUCED PENILE DOPPLER ULTRASOUND DATA

Erectile dysfunction (ED) is a common clinical condition that affects 10-20% of the male population. Penile color Doppler ultrasound (PDUS) is considered as the most objective erection evaluation method, which solely relies on the average blood flow passing through the cavernosal arteries during systole and diastole of the heart. However, this method is somewhat invasive and its diagnostic accuracy is inadequate due to the lack of intracavernosal pressure (ICP) measurement, which is the most precise and direct evaluation parameter of erectile function. On the other hand, highly invasive cavernosometry test is the only measurement method for the ICP. Therefore, a pulsatile lumped parameter model of penile circulation system is developed and coupled to the patient-specific bi-ventricular circulation system to predict the erectile function including the penile pressures and volumes of the system quantitatively and noninvasively. The proposed model is validated by the pre-and post-papaverine injection PDUS and ICP data of 4 ED complaint patients. The numerical model provides detailed hemodynamic information through the employed sensitivity study for both penile erection and bi-ventricular circulation parameters. Moreover, for the diseased patients studied the model predicts the ICP noninvasively with an average error value of 3 mmHg for both pre-and post-injection phases. In addition, penile size change during the phases of erection is simulated with approximately 15% error, according to the clinical penile size measurements. As a result, the developed mathematical model has a potential to be used as an effective non-invasive tool in patient-specific erectile function evaluation, expanding the existing clinical decision parameters significantly.

ÖZET

PENİL EREKSİYON MEKANİZMASININ KISITLI PENİL DOPPLER ULTRASON VERİSİNE GÖRE HASTA BAZLI LUMP PARAMETRE MODELİ

Erektil disfonksiyon (ED), erkek nüfusunun %10-20'sini etkileyen bir hastalıktır. Kalbin sistol ve diyastol hareketi sırasında kanın kavernozal arterlerden ortalama geçiş hızını ölçen renkli penil Doppler ultrason (PDUS) testi, günmüzde erektil disfonksiyonun en objektif değerlendirilme metodudur. Fakat bu klinik uygulama bir miktar da olsa invazivdir ve ereksiyonun en kesin ve direkt ölçüm parametresi olan intrakavernöz basıncı ölçemediğinden bazı uygulamalarda teşhis açısından yetersiz kalmaktadır. Öte yandan, son derece girişimsel bir test olan kavernozometri, intrakavernöz basıncın (IKB) yegane ölçüm metodudur. Bu yüzden IKB ve penil hacim değerlerini girişimsel olmayan bir şekilde hesaplayan bir erektil fonksiyon oluşturmak adına, penil ereksiyon mekanizması toplu parametre yöntemi ile modellenerek bi-ventrikül dolaşım sistemine entegre edilmiştir. Oluşturulan model, papaverine (suni ereksiyon yaratılmasını sağlayan vazodilatör bir ilaç) enjeksiyonu öncesi ve sonrası evreleri için 4 farklı hastadan alınan Doppler ve IKB verileri ile doğrulanmıştır. Bu model kapsamında kullanılan değişkenlerin, modelin hem penil ereksiyon hem de bi-ventrikül dolaşım parametrelerine olan etkileri için bir hassasiyet analizi yapılmıştır. Test yapılan hastalarda IKB 3 mmHg hata değeri ile girişimsel olmayan bir şekilde model tarafından tahmin edilmiştir. Buna ek olarak, ereksiyon esnasındaki penil hacim değişimi de klinik ölçümlere göre yaklaşık olarak %15 hata ile simüle edilmiştir. Sonuç olarak, bu tez kapsamında önerilen matematiksel model ED değerlendirilmesinde kullanılan güncel klinik parametreleri önemli ölçüde genişletmesi açısından, gelecekte bu hastalığın daha kesin ve girişimsel olmayan yollarla değerlendirilmesinde kullanılacak potansiyel bir araçtır.

TABLE OF CONTENTS

LIST OF FIGURES

LIST OF TABLES

LIST OF SYMBOLS

$A_{cav,left}$	Left corpus cavernosum cross sectional area
$A_{cav,right}$	Right corpus cavernosum cross sectional area
C	Compliance parameter
C_{cav}	Cavernosal arterial compliance
C_{corp}	Corpus cavernosum compliance
C_{sa}	Systemic arterial compliance
C_{sv}	Systemic arterial compliance
C_{ven}	Penile venules compliance
$\tilde{D}$	Measured dependent variables of the one step optimization
$D(x)$	Simulated dependent variables of the one step optimization
$D_{cav,left}$	Left cavernosal artery diameter
$D_{cav,right}$	Right cavernosal artery diameter
$\tilde{E}$	Measured dependent variables of optimization step (1)
$E(x)$	Simulated dependent variables of optimization step (1)
$\tilde{F}$	Measured dependent variables of optimization step (2)
$F(x)$	Simulated dependent variables of optimization step (2)
$f_1(x)$	Objective function for step (1) of the two-step optimization
$f_2(y)$	Objective function for step (2) of the two-step optimization
$g(x)$	Objective function for the one step optimization
L	Blood inertia
L_v	Vessel length
P	Blood pressure
P^*	Hydrostatic pressure
P_{corp}	Intracavernosal pressure
$P_{sa(diastol)}$	Diastolic systemic pressure
$P_{sa(systol)}$	Systolic systemic pressure
Q	Time-averaged flow rate
$Q_{cav(diastol)}$	Diastolic cavernosal artery flow rate

$Q_{cav(systol)}$	Systolic cavernosal artery flow rate
r	Vessel radius
R	Vascular peripheral resistance
R_{cav}	Cavernosal arteries peripheral resistance
R_{hel}	Helicine arteries peripheral resistance
R_{out}	Systemic venous resistance
R_{pul}	Pulmonary vascular resistance
$R_{pv,out}$	Penile venules resistance
R_{sys}	Total systemic vascular resistance
R_{sys-l}	Lower body vascular resistance
R_{sys-u}	Upper body vascular resistance
t	Time
V	Chamber volume
V^0	Initial (flaccid) volume
V_{corp}	Corpora cavernosa volume
V^0_{corp}	Flaccid phase volume of corpora cavernosa
V^e_{corp}	Erect phase volume of corpora cavernosa
V_{ven}	Penile venules volume
V^0_{ven}	Flaccid phase volume of penile venules
V^e_{ven}	Erect phase volume of penile venules
x	Parameters to be optimized in step (1)
y	Parameters to be optimized in step (2)
Z_c	Characteristic impedance
Δ	Quantity change of a variable or a parameter
ε	Convergence point for the optimization
μ	Kinematic viscosity

LIST OF ACRONYMS/ABBREVIATIONS

0D	Dimensionless
1D	One Dimensional
2D	Two Dimensional
3D	Three Dimensional
CO	Cardiac Output
CVS	Cardiovascular System
ED	Erectile Dysfunction
EDV	End Diastolic Velocity
ICP	Intracavernosal Pressure
IRB	Institutional Review Board
LA	Left Atrium
LB	Lower Bound
LPM	Lumped Parameter Model
LV	Left Ventricle
PA	Pulmonary Artery
PDUS	Penile Color Doppler Ultrasound
PSV	Peak Systolic Velocity
PV	Pulmonary Vein
RA	Right Atrium
RV	Right Ventricle
SA	Systemic Artery
SV	Systemic Vein
UB	Upper Bound
WK	Windkessel
WU	Woods Unit

1. INTRODUCTION

1.1. Cardiovascular System

Cardiovascular system (CVS) is a mechanical and biological system, which is comprised of a logistic blood circulation network transporting the required nutrients and vital gases to the cells/tissues and collecting waste products. It basically consists of 4 main components: heart (two atria and two ventricles), systemic circulation (upper and lower body blood vessels), pulmonary circulation (blood vessels in lungs) and control system (ensures that the different parts of the body operate in harmony) [1].

Heart is the most important component among these, which starts the CVS from the ventricles and ends it at atria. It pumps the oxygenated and deoxygenated blood to the systemic and pulmonary circuits, respectively by isovolumic relaxations (blood coming from the circuits fills to the atria) and contractions (blood in the ventricles is ejected to the circuits). Blood flow in the heart is governed by the valves which prevent the backward flow of blood between the chambers. There are 2 main valve connections between chambers; mitral valve connects the left atrium to the left ventricle, while the tricuspid valve connects the right atrium to the right ventricle as seen in Figure 1.1.

Blood circulation in the CVS is accomplished through 2 different circuits, which are shown as Figure 1.2. In systemic circulation, O_2-rich blood is transmitted to the organs by the left ventricle and travels back to the right atrium as O_2 poor. On the other hand, in pulmonary circulation O_2-poor blood is pumped to the lungs by the left atrium to take the oxygen from the air breathed and release the CO_2, which is brought from the systemic circulation. Approximately a total of 5.2 liters of blood flows through both systemic and pulmonary circulations per minute [3].

In CVS and oxygen transportation, 3 main types of vessels can be mentioned: arteries, which transmit blood from heart to the organs; veins, which deliver the blood

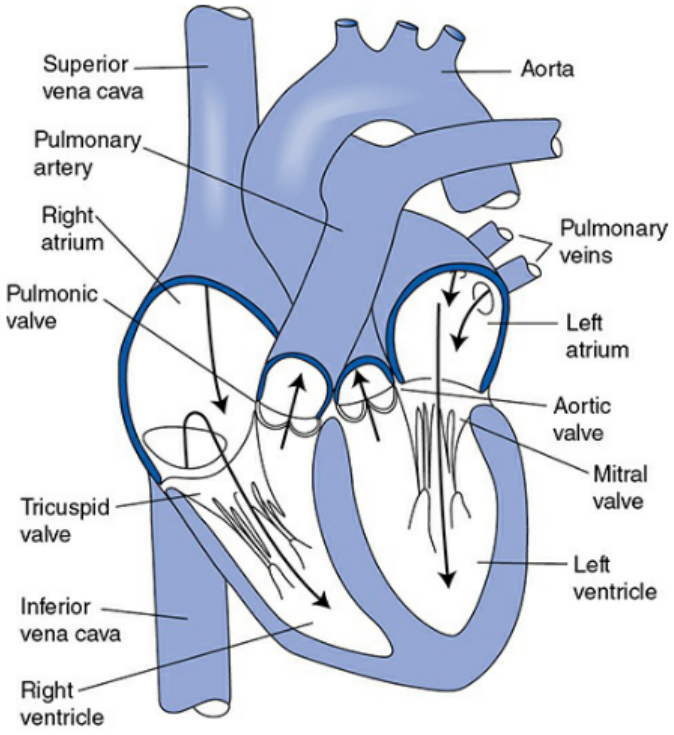

Figure 1.1. Blood flow through the heart valves, main arteries and veins [2]

from organs to the heart and arterioles/capillaries, which ensure the O_2 and CO_2 transfer in the organs and lungs [4].

All arteries in human body are branched from the biggest artery called the aorta, which receives the oxygenated blood from the left ventricle through the aortic valve. After the O_2-rich blood is circulated at the systemic circulation, deoxygenated blood coming from the organs is collected at the veins and conveyed to the right atrium through the main upper and lower body veins; superior and inferior vena cava, respectively. On the other hand, in pulmonary circulation; O_2-poor blood in the right ventricle is transmitted to the lungs through the pulmonary trunk, which receives the blood from the right ventricle through the pulmonary valve. In lungs, gas exchange occurs through the capillaries and after the respiration, capillaries unite to construct the pulmonary vein, which delivers the O_2-rich blood to the left atrium as in Figure 1.2.

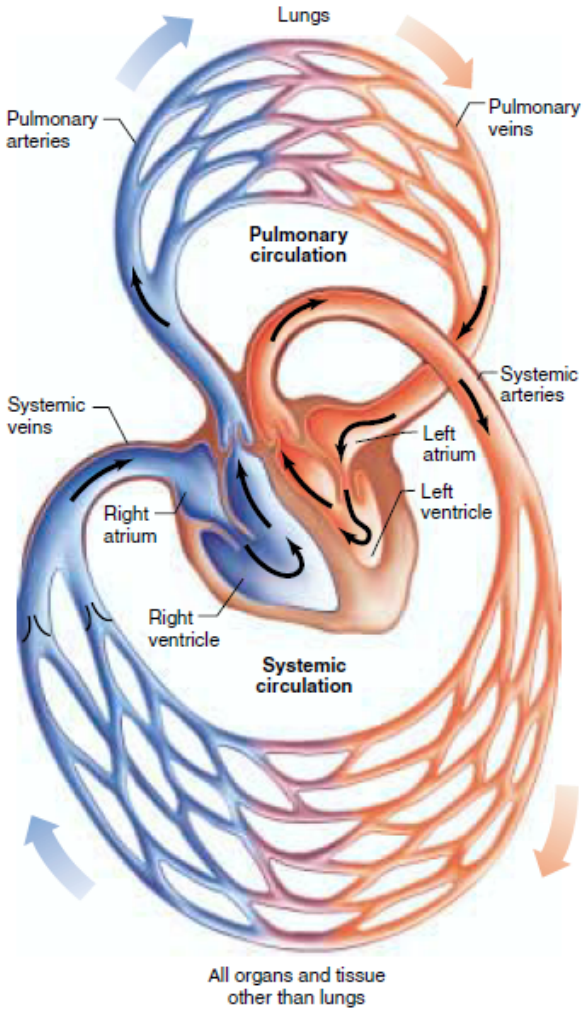

Figure 1.2. Systemic and pulmonary circulations. While the red colored vessels carry the O_2-rich blood, the blue colored ones carry the O_2-poor blood. The color change occurs in the organs, tissues and the lung due to the gas exchange in such systems [5]

Many cardiovascular diseases are closely associated with the blood flow characteristics depending on the shear rate in blood vessels [6]. Although, blood is a non-Newtonian fluid, it behaves like a Newtonian fluid when the shear rate of the vessel is above 100 s^{-1} [7]. Therefore, in large arteries, which has a high shear rate value like aorta, non-Newtonian fluid assumption is invalid and the blood can be considered a fully Newtonian fluid [8]. Blood flow in a vessel, which is not exposed to any external pressure is governed by the pressure gradient across the vessel segment as shown in Figure 1.3.

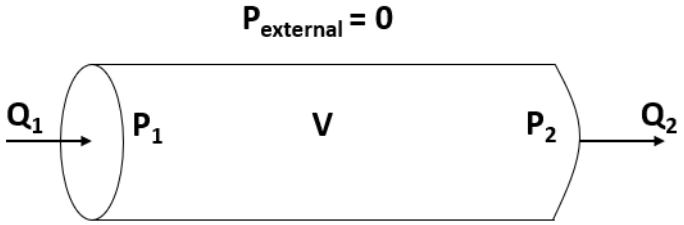

Figure 1.3. Blood flow in an arterial segment [9]

Since flowing blood in an arterial component is highly pulsatile, time averaged flow rate is calculated as;

$$R = \frac{\Delta P}{Q} \tag{1.1}$$

where R is the vascular resistance due to the viscous shear stress of the vessel, ΔP is the pressure difference between two segments of the vessel and Q is the time-averaged flow rate. Vascular peripheral resistance in here is calculated through the following equation which is derived from the Hagen-Poiseuille relation as;

$$R = \frac{8\mu L_v}{\pi r^4} \tag{1.2}$$

where μ is the dynamic fluid viscosity, L_v is the length of the vessel segment and r is the radius of the vessel. Vascular compliance is another important parameter that governs the blood flow in a vessel. It basically represents the volume change of the vessel under a certain pressure, which means the measure of the stretchability of a vessel. Vascular compliance of a circulation element is defined as;

$$C = \frac{\Delta V}{\Delta P} \tag{1.3}$$

where ΔV is the volume change of the element under pressure change ΔP. Understanding the significant parameters that govern the blood flow in human CVS is very crucial since such information provide a basis to develop mathematical models which assist

the clinicians for early diagnosis and/or treatment of cardiovascular related diseases.

1.2. Erectile Dysfunction (ED)

Erectile dysfunction (ED), which is also known as impotence, is a widespread health problem that affects the quality of life throughout the world. It has been reported recently that over 30 million people suffer from ED in the United States; primarily men older than 40 years of age, resulting major socio-economic problems [10]. Moreover, the prevalence of ED is expected to raise considerably, impacting more than 300 million men by 2025 [11]. Therefore, fundamental understanding of the human penile erection mechanism, which is governed by multiple physiological systems in coordination is important. Etiology (cause) of ED can be psychological or physiological. Physiological causes of ED are mainly linked to the cardiovascular diseases such as arterial insufficiency, which is the insufficient blood flow into the penis during erection or venous leakage, which is the inability to keep enough blood in penis to have a sustainable erection. Such etiology of ED represents the 60% of patients as the leading cause and they cannot be generally treated with the vasodilator drugs such as Viagra, Papaverine, Levitra etc. [12, 13] and might require some specific curative surgeries. Therefore, vascular etiologies of ED and their diagnosis/evaluation will be mainly considered in this study.

1.2.1. Erectile Dysfunction Evaluation Methods

There are two main objective quantitative clinical assessment methods of erectile function: penile color Doppler ultrasound (PDUS) and cavernosometry techniques [14]. Doppler ultrasonography is the most common ED evaluation method, which was firstly proposed by Lue *et al.* [15]. They suggested to use the blood flow in cavernosal arteries (there are 2 cavernosal arteries in normal male reproductive system), which are the vessels branching from aorta to deliver the necessary blood to penis, under the effect of papaverine to assess the ED. The regular methodology for PDUS test is based on measuring the peak-systolic (contraction of heart) and end-diastolic (relaxation of heart)

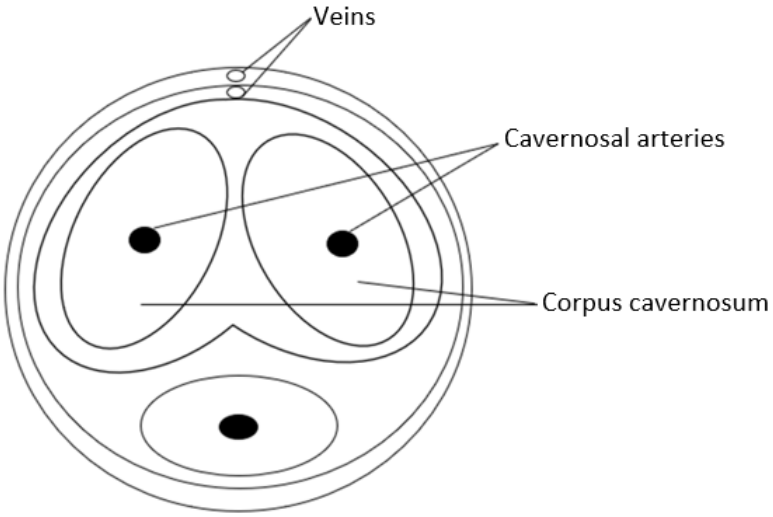

Figure 1.4. Penile erection mechanism main components: cross section view

velocity (PSV-EDV) of both cavernosal arteries flow, their waveform, cavernosal artery and corpora cavernosa (2 corpus cavernosum) dimensions in pre- and post-papaverine injection phases (flaccid and erect phases, respectively). These penile erection mechanism components can be seen in the penis cross section shown in Figure 1.4. Clinicians, mainly radiologists and urologists, observe the right and left cavernosal artery flows and their waveforms separately in different times during the test to evaluate either the ED of patient is physiological or psychological. If PSV<25 cm/s, ED is caused from arterial diseases, mainly arterial insufficiency, whereas EDV>5 cm/s states that venous leakage is the main cause of ED for the patient. [14,16–18]. PDUS is a minimally invasive test due to the intracavernosal papaverine injection and priapism, which is a drug-induced prolonged erection, is the most significant complication of the ED evaluation methods that may be observed in 2.68% of the patients for this procedure [19]. Furthermore, since PDUS test solely relies on average flow rates in cavernosal artery during systole and diastole, its diagnostic accuracy is insufficient for some cases.

The second widespread method, cavernosometry is a highly invasive but a more accurate ED diagnosis technique than the PDUS test. Intracavernosal pressure (ICP), in other words corpus cavernosum (penis) pressure, which is the most appropriate parameter for the direct evaluation of the erectile function can only be measured by

cavernosometry. A needle attached to a pressure sensor is invasively inserted in either one of the corpus cavernosum and ICP is observed in different times during the erection, including pre- and post-papaverine injection phases just like the PDUS test [20–22]. While the literature reported value of a normal male ICP is 10-20 mmHg for flaccid phase, it is nearly 90 mmHg for a full erect penis [23]. Due to the intracavernosal papaverine injection, priapism is also a concern for cavernosometry, which is observed in 13.4% of the patients undergoing this test. Due to its high invasiveness and higher incidence of priapism, cavernosometry is generally preferred by the clinicians only when considering surgical intervention [24].

1.3. Mathematical Modeling of Cardiovascular System

1.3.1. Lumped Parameter Modeling

Mathematical modeling of the human CVS can be divided into 4 main categories: 0D, 1D, 2D and 3D models. While 1D, 2D and 3D models are regarded as distributed parameter models, 0D approximation is called as the lumped parameter model (LPM) which is the main mathematical approach used in this study. Distributed parameter models are generally preferred for the cases, where variation of the blood flow rate in the vessel is important or the complex cases such as blood flow in a bifurcation or a heart valve. However, using such models might be unnecessary and computationally expensive for the studies that investigate only pressure, flow rate and volume in more than one compartmental level [25]. For these cases, LPMs are the more appropriate mathematical approaches to simulate the human cardiovascular system. They are generally preferred to model time-dependent pressure and flow waveforms in any section or a specific condition related to circulation system.

The LPM relies on the analogy between a cardiovascular system and an electric circuit. All hemodynamic elements of the cardiovascular system correspond to the equivalent elements of the electric circuit. Circulation starts from the left ventricle of the heart and blood flows through the vessels of systemic and pulmonary circulation

just like an electrical current. Analogically, just as the current in a circuit is described by Ohm's law, the blood flow in a vessel is described by Poiseuille's law for the steady state flow. Besides, friction due to viscosity, capacitance of the vessels, inertia of the flow, flow rate of the blood and blood pressure in a hemodynamic system are respectively corresponded to the resistance, capacitance, inductance, current and the voltage in an electric circuit [25–27]. The analogy between these two systems can be shown in Table 1.1.

Table 1.1. Hemodynamic system and electric circuit analogous for the important quantities

Hemodynamic system	**Electric circuit**
Blood pressure, P	Voltage, V
Blood flow, Q	Current, I
Blood resistance, R	Electrical resistance, R
Vessel compliance, C	Capacitor's capacitance, C
Vessel volume, V	Charge, q
Blood inertia, L	Inductor's inertance, L
Poiseuille's law: $Q = \frac{\Delta P}{R}$	Ohm's law: $I = \frac{\Delta V}{R}$

Windkessel model (WK) is the simplest expression of the LPM which describes the hemodynamics of the human body. Hales (1735) suggested a model referred as Windkessel that claims the pressure variation in arteries depending on the arterial elasticity. In 1899, Frank [28] formulated the pressure changes in an artery according to resistance and compliance. WK concept, which explains this relationship, is shown in Figure 1.5. While resistance element in the systemic arterial network is the equivalent of the resistance vessels, which are the small arteries and arterioles, capacitor element is comprised of the compliant vessels (windkessels), which are the large arteries. However, there is not a sharp contrast between compliant and resistance vessels, since resistance

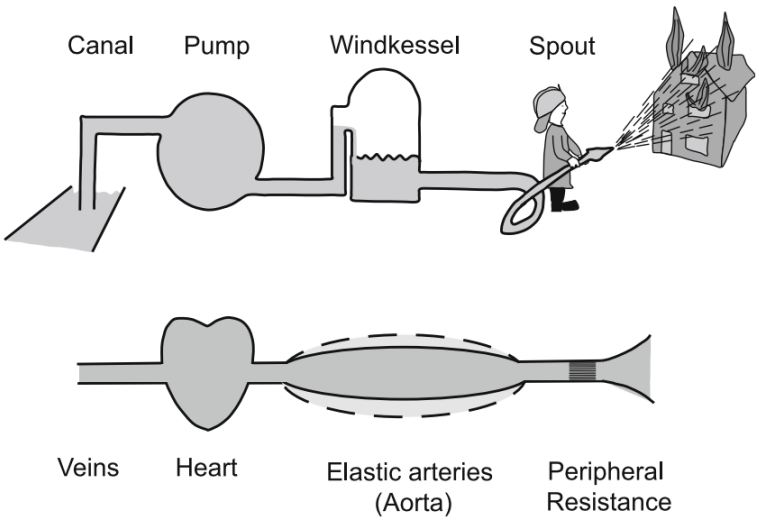

Figure 1.5. The Windkessel approach. Large vessels act like air reservoirs (windkessels) during the systole and diastole of heart [29]

vessels have also some compliant properties and compliant vessels have some resistance [29].

Frank's basic arterial lumped network includes only resistance and compliance, which are connected in parallel with each other to form the 2-element WK model as shown in Figure 1.6a. A 2-element WK model assumes that all arterial elements are lumped in large vessels such as aorta and there is an infinite wave speed in such vessels [30]. Thus, to model cases, which investigate the large vessels, impedance is added to the 2-element WK model as the third parameter [31]. Burratini *et al.* [32] and Westerhof *et al.* [29] are the pioneers who expanded the current network by adding a second resistor, which represents the characteristic impedance (Z_c) in various configurations such as Figure 1.6b and 1.6c. In addition, to determine the arterial compliance more accurate than 2- or 3-element WKs, Stergiopulos *et al.* [33] added a fourth element, which represents the inertia of the blood (L). Since human reproduction mechanism is mainly composed of small arteries and veins, 2 elements (resistances and compliances) are enough to model penile erection mechanism. Therefore, 2-element WKs are used to construct the LPM of penile erection mechanism in our study. The LPMs consider the dependent variables of interest (pressure, volume and flow rate) to be uniformly

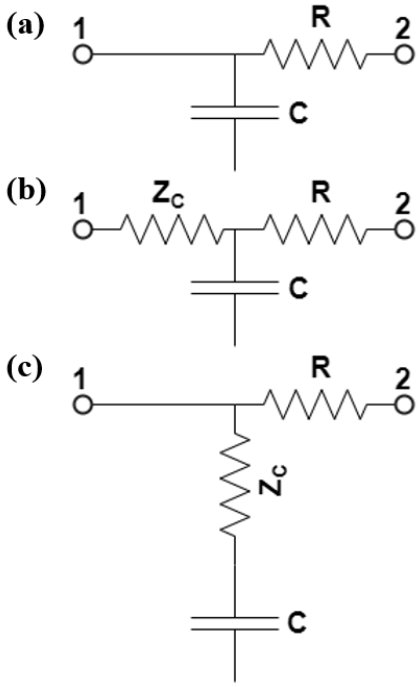

Figure 1.6. 2- and 3-element WK models [25]. (a) 2-element WK model [28] (b) 3-element WK by Westerhof *et al.* [29] (c) 3-element WK by Burratini *et al.* [32]

distributed in a vessel and they are functions of time alone. Thus, a set of ordinary differential equations, which were established by Milisic and Quarteroni [34] to represent the basic laws for blood flow for each element of the system need to be solved to analyze the 2-element and the 3-element LPMs as follows:

$$C\frac{dP_1}{dt} = Q_1 - Q_2 \tag{1.4}$$

$$L\frac{dP_2}{dt} = RQ_2 = Q_1 - Q_2 \tag{1.5}$$

where *1* and *2* indices represent the initial and final value of that quantity, respectively.

1.3.2. Current Literature of Penile Erection Mechanism Modeling

The studies on parameters affecting ED are generally conducted and evaluated based on the clinical data obtained from a group of patients [35, 36], and there are a limited number of studies introducing mathematical models to the literature for explaining the hemodynamic mechanism of penile erection. The content of these studies offered new insight to ED evaluation. Barnea [37] and Borowitz and Barnea [38] developed mathematical models for hemodynamic mechanism of penile erection with lumped and distributed parameters to investigate the ICP, flow rate in corpora (penis) and their relationship under the flaccid and erect phases of erection. The latter study is highly significant since it is the pioneering and the first solid mathematical model that investigates the hemodynamics and the significant parameters of penile erection mechanism. Gillon and Barnea [39] developed another LPM of penile hemodynamics to simulate normal and vascular pathological conditions (arterial insufficiency and venous leakage) for the diagnosis of ED. In their further research, they developed a mathematical model to simulate the cavernosometry test to evaluate venous leakage and elucidate its sensitivity to arterial and venous factors [40]. In addition, Barnea *et al.* [41] developed another model to distinguish the arterial insufficiency and venous leakage and indicate their severity which can be used as a diagnosis tool, by executing an external pressure to trigger the erection. All these mathematical models tried to explain the relation between the pressure and flow rate through the set of differential equations introduced for the LPM.

Besides all these studies that model the penile erection mechanism with lumped parameters, there are some other models in literature that aim to understand the significant parameters of human reproductive system, which were also used for this study. Souper *et al.* [42] investigated the relation between peak systolic velocity and cavernosal artery diameter in the flaccid phase with clinical assessment of erection hardness after intracavernosal injection. They observed that there is no correlation between cavernosal artery diameter in the flaccid phase, and PSV after the injection. Based on their findings, cavernosal artery diameter is assumed nearly constant between

systole and diastole in our study. Chen *et al.* [43] developed a model to identify clinical and engineering parameters of the flaccid penis to predict penile size behavior during erection, without the intracavernosal injection. This study interprets some of the mathematical parameters that govern male erection; however, it does not contain any investigation about the ICP change during erection. Another study on ED, Spessoto *et al.* [35] reported the effect of systemic arterial pressure on ED in patients in initial stages of peripheral arterial disease and they concluded that the progression of ED parallels the development of arterial insufficiency, especially in the initial stages of peripheral arterial disease. Ng *et al.* [44] integrated the bioheat equation to the penile hemodynamic system and observed the temperature difference between flaccid and erect penis, which is mainly aroused by the blood activity flowing into the corpus cavernosum and they concluded that there is 0.1–0.3 ^{0}C difference in blood temperature between the phases of erection. Udelson *et al.* [45, 46] found the values of cavernosal expandability and tunical distensibility during the erection through the engineering approach for buckling, which gives a different perspective for the erection governed by the penile tissue mechanics and properties.

1.4. Objective of Study

Most of the studies covered in the previous section mainly contribute to the better understanding of human penile erection mechanism to improve diagnosis and intervention techniques. As it is understood from the literature, majority of these studies focus on the effect of the penile erection parameters on the reproductive system rather than noninvasive, early and accurate diagnosis of ED.

On the other hand, there are studies which try to mathematically model the penile erection hemodynamics solely rely on the average blood flow passing through the cavernosal arteries during systole and diastole. Since modern clinical ED evaluation methods use the PSV and EDV of blood flowing through cavernosal arteries to evaluate, whether the patient has a vascular-related ED or not, pulsation effect of blood in vessel is very significant and such average based assessment is inadequate in complex

cases. These studies handle the penis as a single compartment, which has an arterial inflow and venous outflow by assuming these flows being not pulsatile but continuous. Moreover, none of them include the main human circulation parameters such as systemic arterial pressure, cardiac output (CO), heart rate and pulsation effect of blood flow to the reproductive system plus the lack of the direct noninvasive calculation of the ICP, which makes them far from clinical applicability. It exposes the need of a more detailed and robust mathematical model which can explain the complicated states of penile erection mechanism by considering all its parameters and pulsation effect.

In this study, a lumped penile erection model was integrated in parallel to the LPM of a normal male bi-ventricle (synchronized movement of the left and right ventricles of heart) circulation, for the noninvasive and accurate prediction of ICP, which is the most significant parameter used to evaluate ED, to overcome the drawbacks of the previous studies.

The lumped parameters (compliances and resistances) used to define the system were estimated through a global least-square optimization algorithm named particle swarm optimization relying on PDUS measurements, which were conducted in Koç University Hospital, so that the ICP can be accurately predicted at any phase of erection.

In addition, to understand the effect of the compliances and resistances of the penile components to the pressure and volume of these elements, a sensitivity analysis has been conducted. Since the exact values of the resistance and compliance parameters have not been studied in the literature before, such analysis have a significance on determining the variables on penile erection mechanism, thus our model has potential to track ED progression through more accessible circulation parameters.

2. LUMPED PARAMETER MODELING OF PENILE ERECTION MECHANISM

2.1. Hemodynamic Model

Hoppensteadt and Peskin [9] modeled the full bi-ventricle normal adult circulation through the most basic lumped parameters, which can be seen in Figure 2.1. However, as it is understood from the same Figure, base LPM framework for the analysis of hemodynamic mechanism of human circulation only includes the heart components with pulmonary vascular resistance (R_{pul}), upper and lower body vascular resistances (R_{sys-u} and R_{sys-l}, respectively). Therefore, even though this network is useful to model some clinical diseases roughly and it demonstrates the basic parameters of LPM, it is not much practical to investigate the human reproductive mechanism or any other organ model specifically. For that, recently established circulatory LPM frameworks for

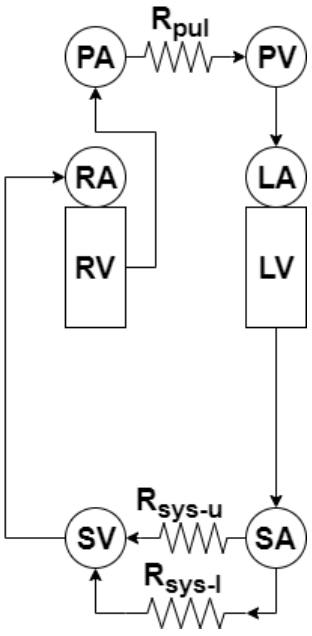

Figure 2.1. Bi-ventricle normal adul circulation by Hoppensteadt and Peskin [9]. LV: left ventricle, RV: right ventricle, LA: left atrium, RA: right atrium, PA: pulmonary artery, PV: pulmonary vein, SA: systemic artery, SV: systemic vein

various clinical cases [47–50] are adopted to develop a network for the penile erection mechanism. Based on these studies, an integrated LPM of penile circulation was considered coupled to the full bi-ventricle normal adult circulation in parallel as given in Figure 2.2. In the improved model, R_{sys-l} is parallelly split up to R_{cav}, R_{hel} and $R_{pv,out}$ to generate another network which can represent the erection model and simulate the erection process appropriately. In normal blood circulation of men, when erection is triggered by brain, average blood flow branching from the systemic circulation (base

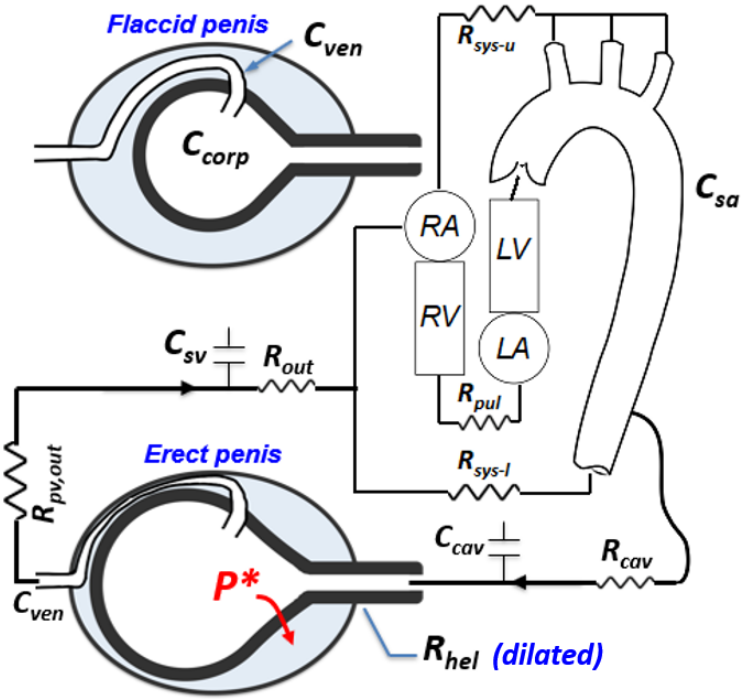

Figure 2.2. The pulsatile lumped parameter circulation network that governs penile erection mechanism. LV: left ventricle, RV: right ventricle, LA: left atrium, RA: right atrium, C_{sa}: systemic arterial compliance, C_{sv}: systemic venous compliance, C_{ven}: penile venules compliance, C_{corp}: corpus cavernosum compliance, C_{cav}: cavernosal arterial compliance, R_{sys-u}: upper body vascular systemic resistance, R_{sys-l}: lower body vascular systemic resistance, R_{pul}: pulmonary vascular resistance, R_{cav}: cavernosal arteries peripheral resistance, R_{hel}: helicine arteries peripheral resistance, $R_{pv,out}$: penile venules resistance, R_{out}: systemic venous resistance. P^* is the hydrostatic pressure that arouse by the increase of ICP, which compresses penile venule to sustain erection.

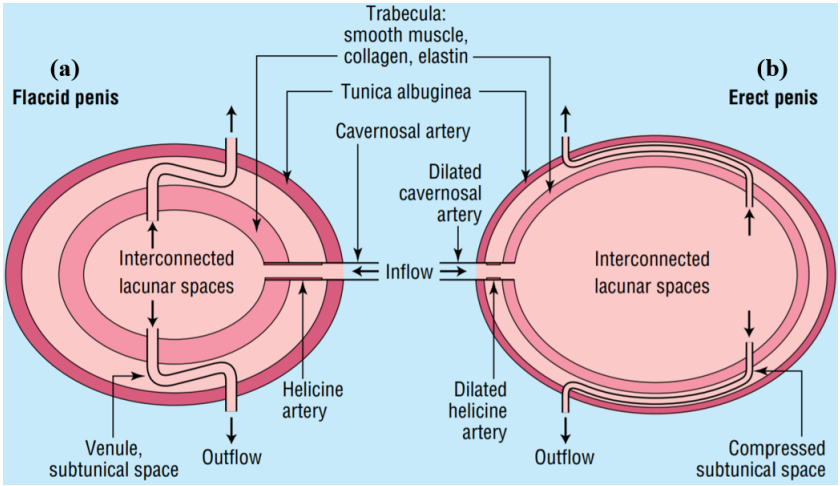

Figure 2.3. Hemodynamic mechanism of penile erection. Anatomical description of our mathematical model [51] (a) Flaccid penis (b) Erect penis

model network) to penile mechanism and filling into the corpus cavernosum lacunar space rapidly increases by the dilation of helicine and cavernosal arteries. In our model, this shift is provided by decreasing R_{cav} and R_{hel} significantly compared to the other parameters, until lacunar space volume reaches its maximum limit, which ensures the closure of penile venules to satisfy the full erect state for a healthy man's erection process. In addition, hydrostatic pressure (P^*) that compresses venules is considered while modeling, which is one of the prominent features of our model. Anatomical description of our LPM and erection process is also shown in Figure 2.3.

The LPM in Figure 2.2 is comprised of 2-element (C and R) WKs. Therefore, to simulate each R-C compartment model, Equation 1.4 was modified to comprise the multi-compartmental models, such as penile erection mechanism, as seen below;

$$\frac{d(CP)_i}{dt} = \sum_{j=1}^{N} \frac{P_j - P_i}{R_{ji}} \tag{2.1}$$

where P and C are the pressures and compliances of the compartments represented by the subscripts i and j. Here, R is the peripheral resistance between the compartments i and j. The order of the subscripts represents the direction of the parameter, namely Q_{ij} means that the flow direction is from compartment i to j. Left hand side of the

Equation 2.1 also represents the rate of the volume change of the relevant compliant chamber.

2.1.1. Flaccid Phase Model

The prediction accuracy of the penile LPM depends on the model design and the values of the lumped parameters such as compliances and resistances that are used to represent the physical system. The parameters for the LPM must be carefully optimized considering the dynamics of the global human circulation. Therefore, a detailed sensitivity study for the flaccid phase of penis is necessary to understand how each compliance and resistance parameter affects each flow rate and pressure. Input parameters of the model (R and C) must be determined to match the PSV and EDV of the blood in cavernosal arteries with the measured systemic pressure and CO for the flaccid penis.

2.1.2. Erect Phase Model

Erection process is accomplished in the model by rapidly decreasing R_{hel} and R_{cav} to allow higher amount of blood flow into the lacunar space (corpus cavernosum). The venule compliant element is compressed with the increasing P^* as a result of the volume extension of lacunar space, as seen in Figure 2.2. This mechanism is imposed to the model through equations relating volume change rate of corpora cavernosa and venule compliant chambers;

$$V^e_{corp} - V^0_{corp} = C_{corp}\Delta P_{corp} \tag{2.2}$$

$$V^e_{ven} = V^0_{ven} - \Delta V_{corp} \tag{2.3}$$

where P_{corp}, C_{corp} and V_{corp} are pressure, compliance and volume of the corpora cavernosa, respectively; while, V_{ven} represents the volume of the penile venules. V^0 is the

flaccid phase volume of the compartment represented by the index and V^e represents the erect phase volume of the same chamber. Δ represents the quantity change of the variable between the phases of erection. Flaccid volume of corpora cavernosa is roughly determined by measuring corpus cavernosum cross-sectional area and penis length in flaccid phase of the patient as suggested by Chen *et al.* [52].

Since the governing parameter of penile erection mechanism is ICP, the most important compliant element for the proposed model is the corpus cavernosum. For this reason, its compliance change during transition from flaccid to erect is included in the model. For some components of the human vascular system, compliance change directed by collagen fibers during blood flow is important [53]. During erection, the collagen fibers in penile erection mechanism are affected by vasodilators synthesized from the chamber perimeters and cause a smooth muscle relaxation, which dilate the lacunar space with the increasing ICP. This feature was imposed to the model through the changing C_{corp} between flaccid and erect phases.

2.2. Numerical Method

As introduced by Hoppensteadt and Peskin [9] and Peskin and Tu [49] *Backward Euler method* was used to solve the governing ordinary differential equation given by Equation 2.1 to obtain the pressure and flow rates of each LPM network element. An implicit formulation using a fixed time step was applied for the iterative solution of the governing equation of the system. The step size is independent from the implicit variables of equation, and one cardiac cycle was divided into 100 time steps. The step size was not changed for different simulations as increasing or decreasing the time step does not have a significant effect on ICP. After the system was waited to reach its steady-state in the flaccid phase, erection was triggered at 6^{th} minute just as the traditional PDUS test, and when system reached its steady-state this time for the erect phase; average, systolic and diastolic flow rates and pressures were acquired for the last few converged cycles to obtain an almost stabilized result.

3. SENSITIVITY ANALYSIS AND OPTIMIZATION

3.1. Sensitivity Analysis

There is no study in literature that reports the compliance and/or resistance values of the LPM of erection mechanism. Therefore, a sensitivity analysis was performed to determine a range for each compliance and resistance parameter for both flaccid and erect phases of penis, to find the patient-specific best parameter set in that range with optimization and to understand the significance of each parameter on ICP and flow rate variables related to penile erection mechanism.

Although there are not any information about the penile erection mechanism and resistances in lierature, main circulation parameters C_{sa}, C_{sv} and total systemic vascular resistance R_{sys} were determined and introduced by Hoppensteadt and Peskin [9]. Order of magnitude of these values were used to identify the base parameter set for our model and sensitivity analysis for these parameters was conducted around these values. However, each compliance and resistance of the base model was divided into many compliant chambers and connected resistances, which constitute the integrated erection model network. Therefore, approximate compliance and resistance values for the flaccid phase of erection model was roughly determined by the research conducted by Goktas *et al.* [54], which investigates the flaccid phase parameters of erection for the ram testicular system. Sensitivity analysis for the erection model parameters were also conducted around the values obtained from their study.

After starting values are roughly determined for each compliance and resistance in flaccid and erect states of erection, each parameter is perturbed by 10% at each simulation one at a time from starting the determined value to evaluate its effects on model outputs, which are P, Q and V values of all elements. Therefore, according to the sensitivities of input parameters on model variables, an appropriate range was determined for all patients to obtain the exact patient-specific parameter set through

the optimization by using the clinical data.

3.1.1. Sensitivity Analysis Results

The sensitivities of the most effective parameters on each erection model variable are presented in Figure 3.1a and Figure 3.1b in the form of Pareto charts, where y-axis stands for the change of the variable with the 10% increase of each input parameter given by x-axis. Although there are total 10 compliances and resistances in our model, only the first 95% of these parameters' cumulative distribution is displayed for both flaccid and erect phases of erection. In addition, since the most effective resistance and compliance parameters on the main circulation variables CO, systolic-diastolic systemic

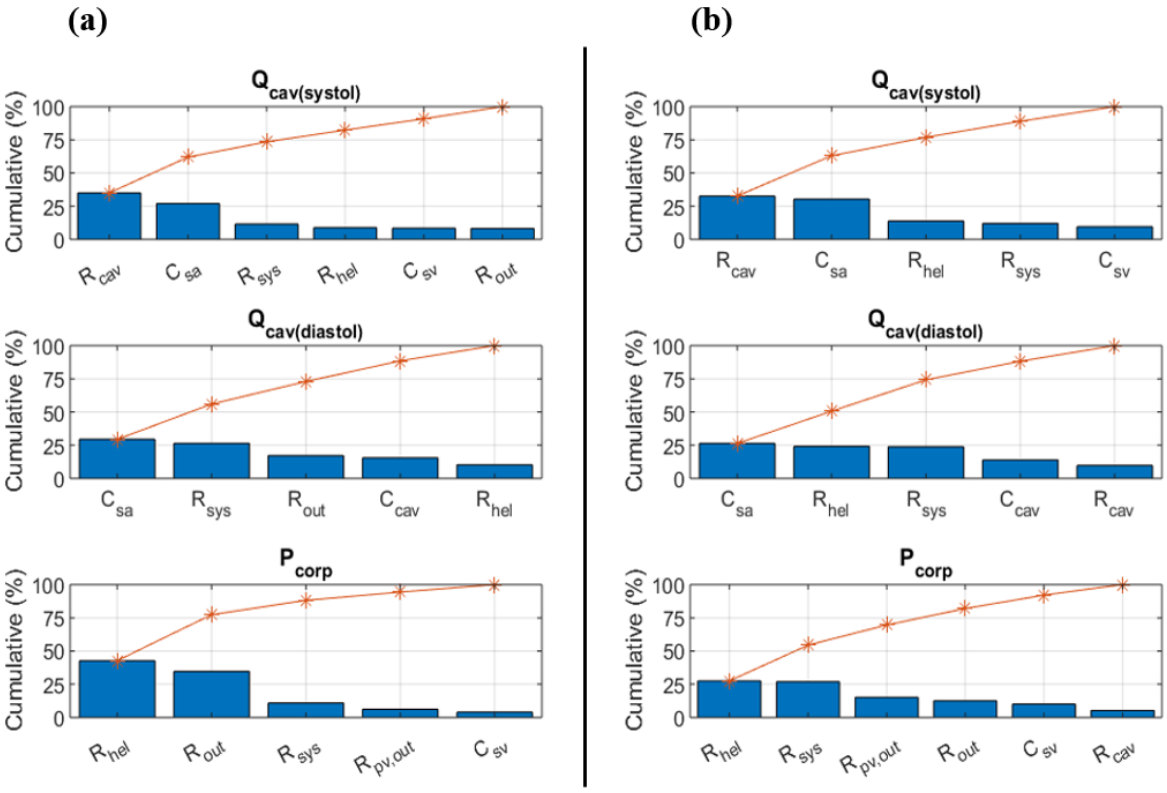

Figure 3.1. (a) Sensitivity analysis for the pre-papaverine injection (flaccid) phase (b) Sensitivity analysis for the post-papaverine injection (erect) phase. $Q_{cav(systol)}$: systolic cavernosal artery flow rate, $Q_{cav(diastol)}$: diastolic cavernosal artery flow rate, P_{corp}: ICP, R_{sys}: total systemic vascular resistance

pressures ($P_{sa(systol)}$ and $P_{sa(diastol)}$, respectively) do not change during transition, their sensitivity are not presented in these figures.

Sensitivity study shows that systolic and diastolic systemic pressures are both sensitive to R_{sys}, C_{sa} and C_{sv} with R_{sys} being the most effective parameter, and this does not change during transition from flaccid to erect phase. However, its effect on systolic and diastolic systemic pressure slightly reduces from flaccid to erect phase. R_{sys}, C_{sa} and C_{sv} are also the most effective parameters on CO, with this time, C_{sv} being the most effective one for both flaccid and erect phases. While R_{hel} is the most effective parameter on P_{corp} in flaccid phase, R_{cav} is added to the effective parameters on ICP in the erect state. On the other hand, the systolic cavernosal artery flow is also sensitive to R_{cav}, R_{hel} and R_{out}, where the former and latter of these parameters have the most significant and limited effect, respectively. Whereas, the diastolic cavernosal artery flow is mostly sensitive to the C_{sa} and R_{sys}, with R_{out}, C_{cav} and R_{hel} have relatively less effect.

3.2. Identification of Model Parameters

As previously mentioned, ICP, which is the most important assesment criterion of erectile function, cannot be measured via PDUS test. Our model enables prediction of ICP by the LPM for flaccid and erect states of penis through the PDUS test measurements. After determination of the input parameter ranges, different potential data sets in that range can be fed to the model to match the PDUS measurements, however, this requires many iterations of trial/error with the chosen parameter sets. Therefore, a least-square minimization method was used to fine tune the input parameters according to the PDUS data and aftermath, the determined best parameter set was used to predict the accurate ICP through LPM for both flaccid and erect phases.

Since determination of the best parameter set is the key step of our study, the most appropriate optimization method must be chosen. Therefore, some global and local optimization algorithms were investigated. When sensitivity of each parameter

to the model variables is investigated separately via the sensitivity study, it is observed that pressure and flow rate outputs are sensitive to compliance and resistance parameters of the network differently. Moreover, all parameters also affect the relevant output differently in different regions of parameter space. Therefore, as there exists multiple local minima in the chosen domain, particle swarm optimization, which is a global optimization algorithm was used to skip the local optima and find the global one, rather than a gradient-based method. The particle swarm optimization function in MATLAB^{TM} Global Optimization Toolbox was used to determine the optimum parameter set for the compliances and resistances.

3.2.1. Particle Swarm Optimization

Particle swarm optimization is a stochastic global optimization method, which was firstly introduced by Kennedy and Eberhart [55] in 1995. They developed this method by taking inspiration from the food searching movements of bird or fish swarms. Each parameter set is a randomly generated particle, which represents a bird or a fish in a swarm. These particles (birds) of the swarm fly through the bounded search space, which consisted of compliance and resistance parameters to find the best value for the objective functions, that are calculated for all particles in each iteration [56]. Particles move towards to the global optimum solution by following the particle which is nearest to the optimum solution of the current iteration [57]. When the best objective function value of the current iteration is less than the objective function limit, which is predetermined by considering the acceptable error for all parameters and computational time, particle swarm reaches the optimum solution and stops at this iteration.

Defining the appropriate objective function is another key step to find the optimum solution. Objective function was determined to minimize the difference between predicted values by LPM and measured values by PDUS. Since model gives the outputs of these values as a vector, measured values were also represented as follow;

$$\tilde{D} = [\ P_{sa(systol)} \quad P_{sa(diastol)} \quad Q_{cav(systol)} \quad Q_{cav(diastol)} \quad CO\ ]^{\mathrm{T}} \tag{3.1}$$

All these parameters can be measured via routine Doppler procedure, except CO, which was calculated by the body size relationship introduced by Jegier *et al.* [58]. Then, the corresponding vector was created by LPM so that its elements coincided with the same type output variable (pressure or flow rate) of the measured values' vector, which is represented as $D(x)$ in Equation 3.2.

In this context, particle swarm function compares an LPM result to its measured value and decides whether the chosen input parameter set is the optimum solution or not. Swarm size for these calculations was chosen as 20. This means that our erection model function, which calculates the pressures and flow rates of the lumped parameter network elements is executed 20 times at each iteration and the best parameter set among these 20 points is chosen to continue to iterate until the optimum point is reached. Since the measured pressure and flow/velocity values that will be optimized have different order of magnitudes, objective function was constructed by normalizing both vectors' elements by dividing each element of them with the coinciding element of measured data vector, shown as in Equation 3.2;

$$g(x) = \sum_{i=1}^{5} \frac{(D(x)_{\mathrm{i}} - \tilde{D}_{\mathrm{i}})^2}{\tilde{D}_{\mathrm{i}}{}^2} \tag{3.2}$$

where x represents the parameter sets used in the model and i is the corresponding dependent variable of the model.

Although optimizing all model parameters through only one particle swarm optimization step as mentioned above is a working method to predict ICP eventually, it was observed that such method requires a considerable amount of computational time. Time for executing the erection model function that computes ICP for each tested input parameter set lasts nearly 48 seconds. There are 20 function executions in each iteration and it was observed that the particle swarm algorithm determined the best input parameter set in between 500 and 550 iterations, depending on the lower and upper bound choosing accuracy. Thus, the required total time to predict the ICP is determined as nearly 5 days for just one phase of the erection, which is not feasible

considering clinical applicability.

Therefore, to overcome the computational efficiency concerns, another methodology that is majorly based on the sensitivity study was developed. As a result of the nature of LPM networks, it is predictable that pressure outputs are majorly sensitive to the compliance parameters, by contrast flow outputs are more sensitive to the resistance parameters. This foresight precisely matches the results of the sensitivity study, which are given as Pareto charts in Figure 3.1a and 3.1b. Thus, due to the nature of global optimization; it is predicted that optimizing the parameters separately as 2 optimization steps would be more effective than the optimizing them for all 5 outputs at once, in terms of computational time. For this, output vector used in one step optimization (Equation 3.1) was divided into two parts considering both sensitivity study results and practices on LPM network working principle: step (1), optimizing the compliance parameters (C_{sa}, C_{sv}, C_{corp}, C_{ven}) and R_{sys} for the main circulation outputs, which were represented as vector $E(x)$ in Equation 3.3 and step (2), optimizing the resistance parameters (R_{cav}, R_{hel}, $R_{pv,out}$, R_{out}) and C_{cav} for the integrated erection model outputs, which were represented as vector $F(x)$ in Equation 3.4. According to the algorithm, the compliances and the R_{sys} determined in the first step are kept constant in the second step, so that only the parameters, given as y parameter set in the Equation 3.4, that have significant effects on the erection mechanism outputs are optimized in the second step.

$$E(x) = \begin{bmatrix} P_{sa(systol)} & P_{sa(diastol)} & CO \end{bmatrix}^{\mathrm{T}} \tag{3.3}$$

$$F(y) = \begin{bmatrix} Q_{cav(systol)} & Q_{cav(diastol)} \end{bmatrix}^{\mathrm{T}} \tag{3.4}$$

Although CO is a flow variable, it is included to the step (1) of the optimization with the pressures. The main reason of this exception is, CO belongs to the main circulation, thus it is highly sensitive to the common parameters with $P_{sa(systol)}$ and $P_{sa(diastol)}$ according to the results of the sensitivity study. Moreover, R_{sys} affects

$P_{sa(systol)}$, $P_{sa(diastol)}$ and CO in high orders, by contrast to its effect on the other model outputs. Hence, R_{sys} was used as an input parameter for the first step of particle swarm optimization with CO as an output for it as a difference from the input parameters and outputs of the step (2). On the other hand, since C_{cav} has a considerable effect on the erection model flows more than main circulation outputs, it is included to the step (2) of the optimization as different from the other compliance parameters.

Objective function given by Equation 3.2 was also separated into two sub-objective functions to introduce both step (1) and step (2) of the optimization as;

$$f_1(x) = \sum_{i=1}^{3} \frac{(E(x)_{\mathrm{i}} - \tilde{E}_{\mathrm{i}})^2}{\tilde{E}_{\mathrm{i}}^2} \tag{3.5}$$

$$f_2(y) = \sum_{i=1}^{2} \frac{(F(y)_{\mathrm{i}} - \tilde{F}_{\mathrm{i}})^2}{\tilde{F}_{\mathrm{i}}^2} \tag{3.6}$$

respectively, while $\tilde{E}$ represents the measured value vector of step (1) variables, $\tilde{F}$ represents the measured value vector of step (2) variables. On the other hand, x is used for the set of all input parameters and y represents only the parameters (R_{cav}, R_{hel}, $R_{pv,out}$ and R_{out}) will be modified at the second step. Flowchart of all optimization process is given as Figure 3.2 for a better understanding.

As predicted, nearly same optimum parameter sets with the one step method for flaccid and erect phases of erection were determined by two step optimization approach, in only between 70 and 80 iterations per step. Therefore, required total time to predict ICP for the two step optimization method is determined nearly 2 hours, which can be considered an acceptable computation time for such a complex mathematical model.

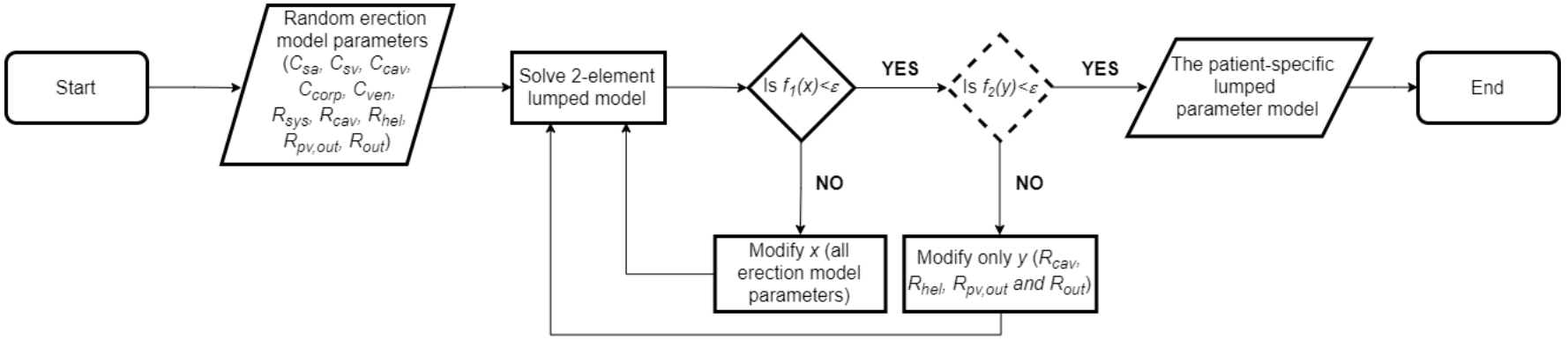

Figure 3.2. Schematic representation of the two-step particle swarm optimization algorithm of penile erection circulation system parameters. The first-step prediction level of this algorithm is indicated via continuous line diamond, while the dashed one represents the second step. Compliance and resistance parameters are randomly generated in each iteration to calculate the $f_1(x)$ and $f_2(y)$ through the objective functions, until the calculated functions are lower than the selected convergence point $\varepsilon = 0.005$, which is the convergence criteria of the objective functions

4. CLINICAL TESTS FOR VALIDATION

As mentioned in previous chapters, both PDUS and cavernosometry tests are the most common ED evaluation methods. Although these tests are pretty much routine procedures and they are well-defined in the clinical guidelines; nonetheless, an approval from an ethics committee is required to use patient data in this study. Therefore, we gained an Institutional Review Board (IRB) approval (protocol no: 2018.237.IRB1.030) from the Koc University Committee on Human Research. In addition, the written informed consent of the patients were obtained. After that, PDUS and cavernosometry tests were simultaneously performed in 4 men with the complaint of ED who were randomly selected between 18-70 years of age. The exclusion criteria for participants as applicable in this study are having a known history of priapism, penile implant, multiple myeloma, leukaemia, atriaventricular block and being allergic to papaverine and/or any other vasoactive medications used during the tests. PDUS and cavernosometry tests were performed in Koc University Hospital. Both tests were performed complying with the existing relevant clinical protocol and took a total of about 30-40 minutes.

In addition to the PDUS and cavernosometry tests, each patient's systolic and diastolic systemic pressures which are 2 of the main circulation outputs of our LPM were observed during the tests. For the other main circulation output, CO, each patient's weight and height were measured before the test to obtain the body surface area through the relation introduced by Du Bois and Du Bois [59]. From the body surface area, CO was simply calculated, as previously mentioned [58].

4.1. Penile Color Doppler Ultrasound (PDUS) Test

Since results of the PDUS test form some part of the outputs of the LPM which are used at the optimization step (2), such data is very important for the effectiveness of the model. All PDUS test data in the literature are presented as the averaged values for a large number of patients, thus we conducted our own clinical experiments to

obtain the penile erection parameters at each phase of erection separately.

In PDUS test, PSV-EDV, corpora cavernosa cross sectional area (both right and left corpus cavernosum) and both right and left cavernosal artery diameters were measured and recorded as the routine of the Doppler procedure. Although only flaccid and erect data of the patients were used in our model, the intermediate phases (latent and tumescent penis) between these two stages were also measured to control the accuracy of the test.

While the flaccid phase data of the erection was measured at the initial 5 minutes of the test, data of the subsequent phases were measured at 10^{th}, 15^{th} and 20^{th} minutes of the test, respectively, to represent all four phases. Once the flaccid phase data was measured, each patient was injected with 60 mg papaverine, again as the routine procedure of the test, and same parameters were measured for the rest 3 phases.

All parameters were meaured via LOGIQ S8 (GE Healthcare, Milwaukee, WI) ultrasound machine with an ML6-15 linear array probe, which are given as Figure 4.1a

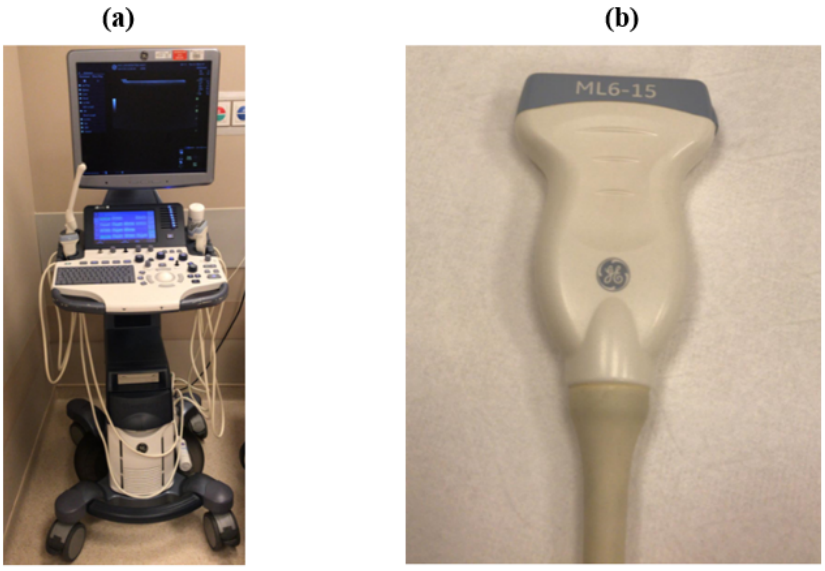

Figure 4.1. (a) LOGIQ S8 color Doppler ultrasound machine (b) ML6-15 linear array probe

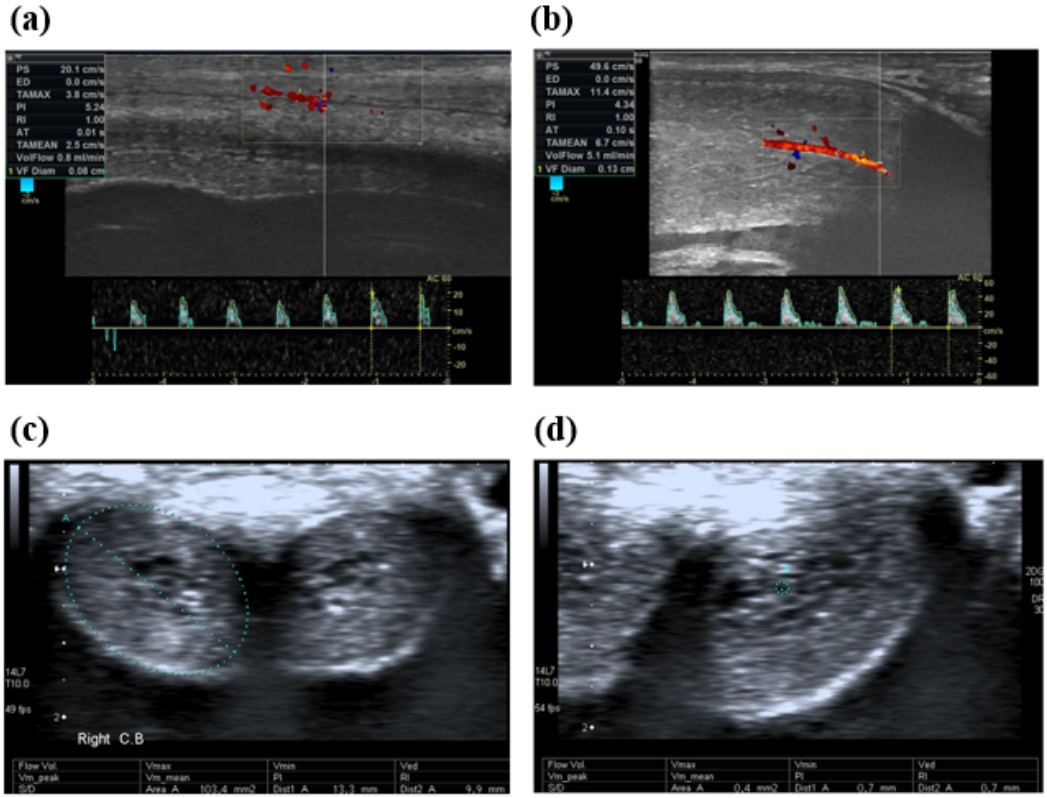

Figure 4.2. (a) Doppler trace of PSV-EDV acquired from the left cavernosal artery during the flaccid (pre-injection) phase of *Patient 2* (b) 10^{th} minute after injection (stimulated) Doppler observation of PSV-EDV in left cavernosal artery of *Patient 3* (c) Right corpora cavernosa dimensions measurement for *Patient 1* (d) Left cavernosal artery dimensions measurement for *Patient 4*

and Figure 4.1b, respectively. Some of the chosen Doppler observations are given in Figure 4.2a, 4.2b, 4.2c and 4.2d.

4.2. Cavernosometry Test

Cavernosometry test was applied to the patients simultaneously with the PDUS test since papaverine injection is also required in this test to eliminate the psychological effects preventing erection. The test was conducted by following the times of the Doppler procedure but this time to measure the ICP. A specifically developed and integrated pressure sensor, which is shown in Figure 4.3, was used to measure the

Figure 4.3. The pressure sensor which was placed to the patient corpus cavernosum to measure the ICP during the phases of erection

pressure in either one of the corpus cavernosum. The measured data was transferred to the computer and monitored via a LabVİEW platform, which was previously written. Since both right and left corpus cavernosum pressures increase together during erection, ICPs of the both right and left chambers are assumed nearly equal. Moreover, since the placement of the pressure sensor in either of corpus cavernosum was practised with a winged infusion set (butterfly needle), it is not much comfortable for the patients to obtain data from both chambers. Since continuous measurement of ICP requires that the placement of pressure sensor precisely by providing only a little movement of the needle in either of corpus cavernosum during the tests, it is considerably difficult for patients to achieve the full erect status. Therefore, in this study, flaccid phase and the reached maximum ICP values were used to validate our mathematical model's pre- and post-injection simulations. A sample ICP change during the erection process of *Patient 1* is shown in Figure 4.4.

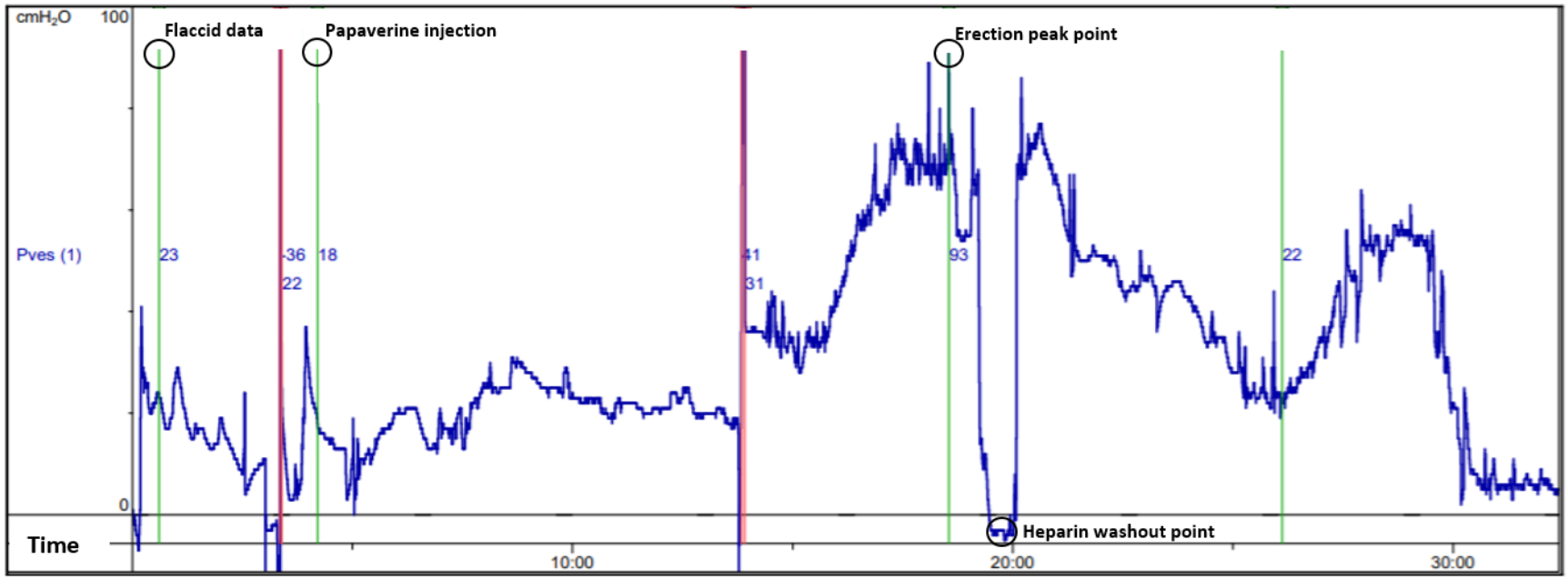

Figure 4.4. Sample cavernosometry trace which represents the ICP during the erection for *Patient 1.* In addition, since heparin washout is used to test for the pipes of the infusion set, a significant decrease in ICP is observed at that point

5. RESULTS AND DISCUSSION

5.1. LPM Results and Validation

5.1.1. Penile Erection Mechanism

As discussed in previous chapters, the mathematical model uses the main circulation parameters ($P_{sa(systol)}$, $P_{sa(diastol)}$ and CO) and PDUS measurements ($Q_{cav(systol)}$ and $Q_{cav(diastol)}$) to find the optimum parameter set, which satisfies these outputs for the relevant patient. This procedure was applied by defining an objective function for particle swarm optimization composed of these variables, and the optimum compliance and resistance set that minimizes the objective function was determined. Using the optimized parameter set of compliance and resistances based on the measured values, ICP was predicted for pre-and post-injection phases for all patients. Table 5.1 and Table 5.2 represent the tuned measurement values and the predicted ICP for the pre- and post-papaverine injection, respectively. On the other hand, Table 5.3 represents the predicted and measured ICP values for validation for all patients.

Table 5.1. Comparison of the penile color Doppler ultrasound (PDUS) measurements vs. lumped parameter modeling (LPM) predictions are presented corresponding to the pre-injection phase for *Patient 1*

	PDUS	**LPM**
$P_{sa(systol)}/P_{sa(diastol)}$ *(mmHg)*	135/81	135/81
CO (lt/min)	7.60	7.59
$Q_{cav(systol)}$ *(lt/min)*	0.0105	0.0105
$Q_{cav(diastol)}$ *(lt/min)*	∼0	∼0
ICP (mmHg)	**11.05**	**13.17**

Table 5.2. Comparison of the penile color Doppler ultrasound (PDUS) measurements vs. lumped parameter modeling (LPM) predictions are presented corresponding to the post-injection phase for *Patient 1*

	PDUS	**LPM**
$P_{sa(systol)}/P_{sa(diastol)}$ *(mmHg)*	135/81	135/81
CO (lt/min)	7.60	7.58
$Q_{cav(systol)}$ *(lt/min)*	0.0632	0.0630
$Q_{cav(diastol)}$ *(lt/min)*	-0.0016	-0.0016
ICP (mmHg)	**68.4**	**63.7**

Table 5.3. Predicted and measured intracavernosal pressure (ICP) levels for all patients. Pressure values are tabulated in $mmHg$ for pre-and post-injection phases

	Pre-injection		**Post-injection**	
Patient no	**Clinical measurement**	**Model prediction**	**Clinical measurement**	**Model prediction**
1	11.05	13.17	68.40	63.65
2	11.80	10.22	65.20	57.44
3	10.20	9.50	52	56.58
4	12.02	11.27	Not applicable	Not applicable

As it is seen, ICP can be predicted with an average error value of 3 mmHg by our model. Our model approximates the cavernosal artery and corpus cavernosum as one compliant chamber; thus, flow rates in tables represent the total flow rate through cavernosal arteries. *Patient 4* did not react to papaverine injection significantly and could not maintain the erection. Therefore, only pre-injection ICP could be predicted

and compared with the clinical data for this patient.

5.1.2. Flow Waveform

Since the developed mathematical model include the flow pulsatility, an expanded set of hemodynamic parameters can be predicted compared to the earlier models in literature [37–41]. For example, the measured and simulated waveforms of cavernosal artery flow in post-injection state can now be compared. Doppler waveform measured and observed by Halls *et al.* [14] was used for the evaluation of our simulated waveform, as shown in Figure 5.1. Since the PDUS data of each patient is different, the systolic and diastolic cavernosal artery flow rates obtained from our LPM were scaled according to the EDV and PSV measured by Halls *et al.* [14] to compare waveforms. Our model simulates the erection mechanism as a simple loop rather than 2 parallel loops and right and left cavernosal artery flows were not approached separately. On the other hand, $Q_{cav(systol)}$ and $Q_{cav(diastol)}$ were roughly scaled to represent only one of the cavernosal arteries. Therefore, our model considers the pulsation of a single cavernosal artery flow. As a result, the differences observed in pulsation and systolic times between Doppler waveform and our LPM model are 0.14 seconds and 0.023 seconds, respectively.

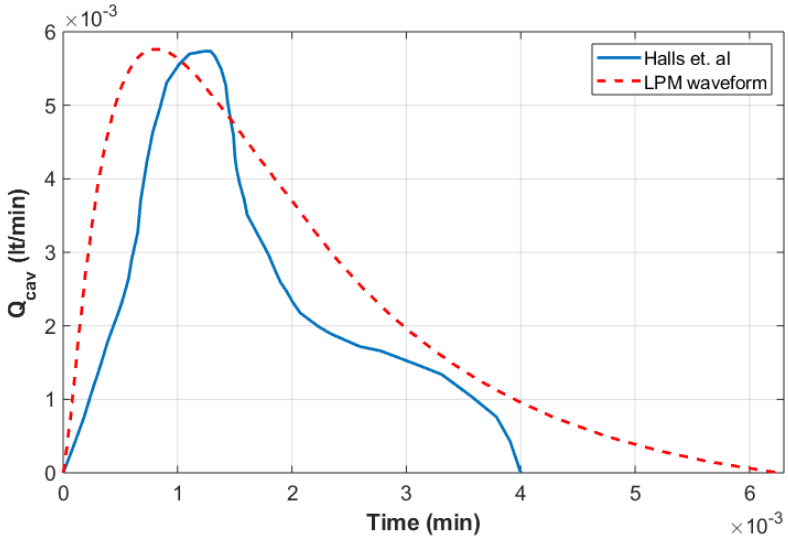

Figure 5.1. Waveform comparison of simulated and measured cavernosal artery flow after the papaverine injection

5.1.3. ICP and Penile Volume Change

Measured ICP data during transition from flaccid to erect is subject to significant noise due to the practical difficulties of reaching and maintaining the erect phase in clinical environment. Whereas, our model assumes that after the erection is triggered, erection process is not interrupted or stopped, as presented in Figure 5.2a. Therefore, predicted ICP can only be validated during the measured ICP, at a certain time. Figure 5.2b shows that ICP increases to 64 mmHg from flaccid corporeal pressure (∼13 mmHg) in nearly 2.5 minutes for the *Patient 1*. After LPM system has reached its steady-state, erection was triggered at 4^{th} minute and the erect state was reached at 6^{th}-7^{th} minute. While corpus cavernosum volume increases with the increasing ICP on subtunical space and penile venules gradually, penile venules tighten to allow the outflow of a very small portion of the blood in the penis, which ensures to obtain and sustain the erection.

Relation between V_{corp} and V_{ven} during erection was also investigated in this study, as shown in Figure 5.2b. Flaccid and erect volumes of corpora cavernosa (V^0_{corp} and

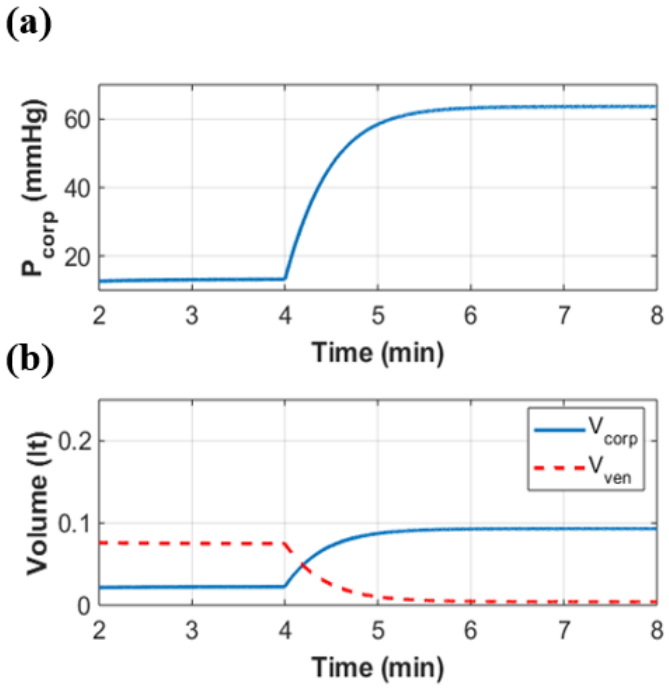

Figure 5.2. (a) ICP change during erection (b) Penile size change during erection

V_{corp}, respectively) were calculated as 0.019 lt and 0.11 lt, by using the measured corpus cavernosum cross-sectional area and penis length based on the relation introduced by Chen *et al.* [52] and Nelson and Lue [60]. Whereas, V^0_{corp} and V_{corp} were predicted through the LPM as 0.023 lt and 0.10 lt, respectively. Therefore, it can be seen that as the blood fills into the lacunar space, it enlarges to ∼4 times of its flaccid volume by gradually compressing penile venules. Our model can predict such enlargement of corpora cavernosa (penis) within acceptable ∼85% accuracy.

5.1.4. Main Circulation Parameters and Cavernosal Artery Flow

Since penile erection mechanism is integrated to the main human circulation in our LPM network, pulsating main circulation parameters; systemic pressure and CO changes during erection were also simulated with erection being triggered at a specific

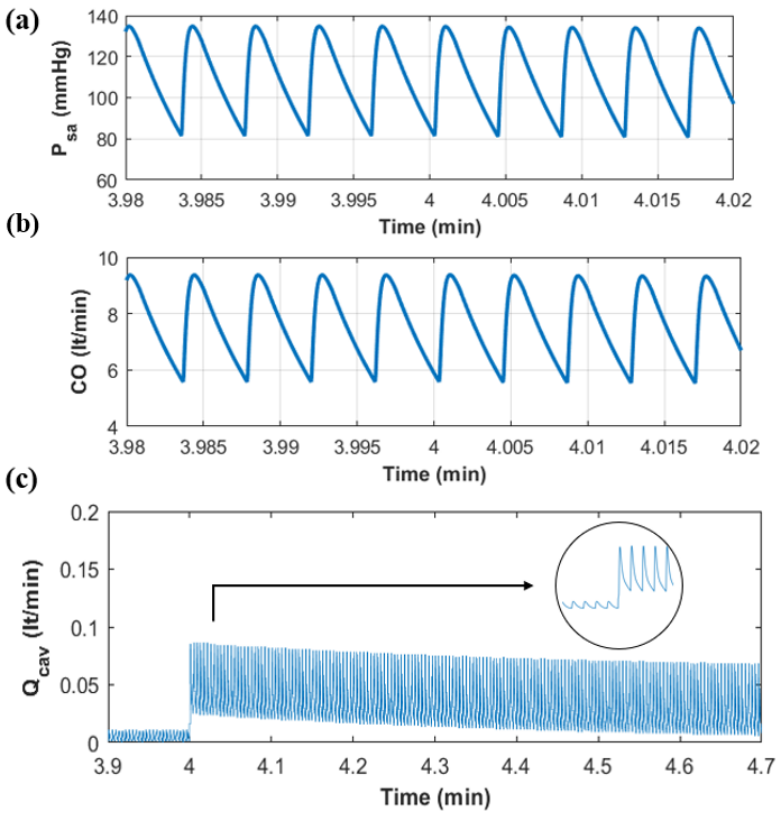

Figure 5.3. (a) Systemic pressure change during erection (b) Cardiac output (c) Cavernosal artery flow during erection

time, as shown in Figures 5.3a and 5.3b. Trends in computed cavernosal artery flow rate during the erection phases are plotted in Figure 5.3c as a function of time. Erection was triggered exactly at the set time of 4^{th} minute and cavernosal artery flow rate into penile lacunar space rapidly increases with the effect of papaverine on R_{cav} and R_{hel}, and it gradually decreases until post-injection ICP was provided in steady-state. On the other hand, main circulation parameters (systemic pressure and CO) remain nearly constant during erection.

5.2. Discussion

This study suggests that 2-element (compliances and resistances) LPM can be used to model and simulate the pulsatile flow and pressure dynamics during human penile erection mechanism patient-specifically. The most clinical feature of such a model is the determination of the optimum compliance and resistance values. As the present study shows, main circulation parameters influence the clinical condition at varying levels of sensitivity. Both for the flaccid and erect phases, a successful automated tuning of PDUS test data is achieved for 4 ED patient cases. Therefore, ICP can be predicted through the model for both states similar to a cavernosometry test. As a result, patient-specific ICP can be predicted within a certain error range for all patients for both pre- and post-injection of papaverine, as given in Table 5.3. Error difference in ICP predictions among patients mainly arouse from the deviations in determining the optimization range for different patients.

In order to execute a successful optimization, a detailed sensitivity study was conducted to observe the effects of the compliance and resistances on the system, as sketched in Figures 3.1a and 3.1b. The most important outcome of this sensitivity analysis is the dependency of ICP during erection to the peripheral resistances of helicine arteries. Interestingly, we found that the corporeal compliance does not have any significant effect on ICP during transition from flaccid to erect, which is coherent considering the dynamics of the mechanism. That significant outcome of our study also corresponds to the physiological features of the erection elaborated in clinical

studies [11, 61, 62].

The investigated cavernosal artery velocity waveform gradually turns into the lanceolate waves during erection; however, our model cannot accurately reflect this change and our pulsatile waveforms are mostly in accordance with the post-papaverine injection state waveforms obtained from the clinical tests. Therefore, our LPM waveform was compared to the erect state measurements obtained by PDUS technique, which were reported by Halls *et al.* [14] and similar waveforms were observed with acceptable deviation.

Intracavernosal pressure (ICP) was calculated by using the general governing equation for lumped circulation network represented by Equation 2.1. It can be seen from the Figure 5.2a, the increase of ICP is exponential. The main reason of this trend is; C_{corp} decrease during the transition from flaccid to erect, which is directed by the contraction of the ischiocavernous muscle [53].

Systemic pressure and CO pulsation behavior and their changes during erection were also simulated in this study, which was shown in Figure 5.3. It can be observed that average values of pulsating systemic pressure and CO remain nearly constant during transition from flaccid to erect, which is consistent with the results of Lue *et al.* [61]. These results enable clinicians to observe the change of main circulation parameters during erection, which can be used to control the accuracy of the simulation.

Simulating the volume changes of the erection lumped network components by using the lacunar space hydrostatic pressure effect on the venule compression is another prominent feature of the proposed model. Since V_{corp} and V_{ven} compose an integrated structure for the penile hemodynamic mechanism by enlarging and tightening together during erection as shown in Figure 2.2, total volume of these compliant chambers remains constant during erection, which is also sensible in terms of the physical aspects of the erection. Penile volume predictions are less accurate than the ICP predictions for both pre-and post-injection states, and it is majorly aroused by the deviations in

determining optimized values of C_{corp}, and predicting P_{corp} by LPM for both states of penis, since volume of this component is very sensitive to these two parameters. Volume accuracy can be improved through additional optimization studies in the future.

5.3. Limitations

Penile erection is a complex mechanism that involves several features omitted here. Primarily, our model integrates the right and left corpus cavernosum circulation as one compliant chamber and lumps the right/left cavernosal arteries as one vessel that transports the blood to the erection model. However, if needed, the right and left segments can be separated for specific disease states. In addition, there is not any experimental model in the literature to compare our numerical model. Another important limitation is that, nonlinear stiffening of collagen layers is not included, and all compliant chambers have been accepted as to behave linearly. Heart component is not also very detailed in our LPM. Finally, a robust optimization method must be integrated to the model for identification of the input parameters.

6. CONCLUSIONS AND FUTURE WORK

6.1. Conclusions

ED is one of the most significant clinical cases that affects the life quality of men of different age groups. Although it might be due to psychological reasons, it is generally aroused by some cardiovascular related (physiological) problems. Therefore, many clinical tests, most commonly PDUS and cavernosometry, are conducted to understand whether ED is psychological or physiological. However, since such tests are invasive and inaccurate in some conditions due to their application methods, a different assessment procedure is needed to be developed for ED. For this purpose, we have developed an LPM of penile erection mechanism, which can represent the erection process and simulate the ED evaluation tests in the computer environment.

The developed mathematical model was successfully integrated to the normal bi-ventricle human circulation in the literature. Therefore, through the developed LPM, erection parameters, which are mainly cavernosal artery flow, penile volume and penis pressure, in other words ICP, can be calculated by feeding the appropriate compliance and resistance parameters to the model. The appropriate compliance and resistance values were not determined in any of the previous studies, thus the optimum input parameter set including the compliance and resistance of the penile erection mechanism components was patient-specifically determined in this study, for the first time in literature.

ICP is the most significant evaluation parameter for the erectile function and it is clinically measured by the invasive cavernosometry test. Thus, the main output parameter of our LPM is ICP. To predict the ICP accurately, noninvasively and patient-specifically, we have conducted the routine PDUS test and used the results of the test to tune the model and find the appropriate parameter set for the relevant patient in different phases of erection. The determined data set was fed to the LPM and

by this way ICP and penile component volumes were calculated for pre- and post-injection phases of erection for each patient. The ICP values predicted by the LPM were validated with the conducted cavernosometry tests for pre- and post-injection phases of each patient.

Our LPM includes the blood flow pulsatility and vascular compliance, which enhance the clinical applicability of our model. In addition, by means of such prominent feature, our model can also be generalized and applied to different clinical cases other than ED. Since there are very limited studies that quantify ED in literature, our model validated with unique clinical studies is an important contribution to penile hemodynamics literature. Finally, non-invasively prediction of ICP has a significant potential to be used as an alternative tool for the precision of the evaluation of ED.

6.2. Future Work

Erection model is one of the most complex systems in human body, thus, even though the proposed LPM has taken the literature a step further, there are still potential future works to do.

First of all, as previously discussed, our model approaches the human penis as a single compliant chamber which has a single arterial and venous vessel. Therefore, to investigate the human reproductive system more detailed, corpus cavernosum chambers and cavernosal arteries peripheral resistances can be divided into two parallel networks to represent right and left parts of the system. By this way, since model output variables obtained from PDUS test will increase, required iterations for the optimization to determine the input parameters may be less than the current method. Accordingly, the needed computational time for such work might significantly decrease. In addition, investigating the both parts of the system separately might contribute to the clinicians' decision on the patient in a positive way.

On the other hand, since cavernosometry is a tedious and long-drawn-out procedure, it was applied to only 4 potential ED patients in this study. However, with the providing a large number of patient data to the LPM, a patient characterization might be done in future studies. Therefore, such model can be optimized for all patients which might be beneficial since it can decrease the clinical test number and time not only for the clinicians but also for the patients.

REFERENCES

1. Hall, J. E. and A. C. Guyton, *Textbook of Medical Physiology*, Elsevier Inc., Philedelphia, 13 edn, 2016.

2. Mohrman, D. E. and L. J. Heller, *Cardiovascular Physiology*, McGraw-Hill Education, 9 edn, 2018.

3. Longenbaker, S., *Mader's Understanding: Human Anatomy and Physiology*, McGraw-Hill Education, 5 edn, 2004.

4. Bronzino, J. D., *The Biomedical Engineering Handbook*, Taylor & Francis, 3 edn, Boca Raton, 1995.

5. Vander, A., J. Sherman and D. Luciano, *Human Physiology: The Mechanism of Body Function*, McGraw-Hill, 8 edn, Boston, 2001.

6. Moayeri, M. S. and G. Zendehbudi, "Effects of Elastic Property of the Wall on Flow Characteristics through Arterial Stenoses", *Journal of Biomechanics*, Vol. 36, pp. 525–35, 2003.

7. Berger, S. A. and L.-D. Jou, "Flows in Stenotic Vessels", *Annual Review of Fluid Mechanics*, Vol. 32, pp. 347–82, 2000.

8. Fung, Y. C., *Biomechanics: Circulation*, Springer, 2 edn, New York, 1997.

9. Hoppensteadt, F. C. and C. S. Peskin, *Mathematics in Medicine and Life Sciences*, Springer, New York, 1 edn, 1992.

10. Nunes, K. P. and R. C. Webb, *Erectile Dysfunction - Disease-Associated Mechanisms and Novel Insights into Therapy*, IntechOpen, 2012.

11. Shamloul, R. and H. Ghanem, "Erectile Dysfunction", *Lancet*, Vol. 381, No. 9861, pp. 153–165, 2013.

12. Hafez, E. S. and S. D. Hafez, "Erectile Dysfunction: Anatomical Parameters", *Archives of Andrology*, Vol. 51, pp. 15–31, 2005.

13. Reed-Maldonado, A. B. and T. F. Lue, "A Syndrome of Erectile Dysfunction in Young Men?", *Translational Andrology and Urology*, Vol. 5, pp. 228–234, 2016.

14. Halls, J., G. Bydawell and U. Patel, "Erectile Dysfunction: The Role of Penile Doppler Ultrasound in Diagnosis", *Abdominal Imaging*, Vol. 34, No. 6, pp. 712–725, 2009.

15. Lue, T. F., H. Hricak, K. W. Marich and E. A. Tanagho, "Vasculogenic Impotence Evaluated by High-Resolution Ultrasonography and Pulsed Doppler Spectrum Analysis", *Radiology*, Vol. 155, pp. 777–781, 1985.

16. Bari, V., M. N. Ahmed, M. Z. Rafique, K. Ashraf, W. A. Memon and M. U. Usman, "Evaluation of Erectile Dysfunction with Color Doppler Sonography", *Journal of Pakistan Medical Association*, Vol. 56, pp. 258–261, 2006.

17. Wilkins, C. J., S. Sriprasad and P. S. Sidhu, "Colour Doppler Ultrasound of the Penis", *Clinical Radiology*, Vol. 58, pp. 514–523, 2003.

18. Connolly, J. A., S. Borirakchanyavat and T. F. Lue, "Ultrasound Evaluation of the Penis for Assessment of Impotence", *Journal of Clinical Ultrasound*, Vol. 24, pp. 481–486, 1996.

19. Fuselier, H. A., J. M. Allen, A. Annaloro and J. O. Morgan, "Incidence and Simple Management of Priapism Following Dynamic Infusion Cavernosometry-Cavernosography", *The Southern Medical Journal*, Vol. 86, pp. 1261–1263, 1993.

20. Kaufman, J. M., F. D. Borges, W. P. Fitch, R. A. Geller, M. B. Gruber, J. G.

Hubbard, D. L. McKay Jr., J. P. Tuttle Jr. and F. R. Witten, "Evaluation of Erectile Dysfunction by Dynamic Infusion Cavernosometry and Cavernosography (DICC). Multi-Institutional Study", *Urology*, Vol. 41, pp. 445–451, 1993.

21. Delcour, C. and J. Struyven, "Techniques for Performing Cavernosometry and Cavernosography", *Cardiovascular and Interventional Radiology*, Vol. 11, pp. 211–217, 1988.

22. Vardi, Y., S. Glina, J. P. Mulhall, F. Menchini and R. Munarriz, "Cavernosometry: Is it a Dinosaur?", *Journal of Sexual Medicine*, Vol. 5, pp. 760–764, 2008.

23. Bookstein, J. J., K. Valji, L. Parsons and W. Kessler, "Penile Pharmacocavernosography and Cavernosometry in the Evaluation of Impotence", *Journal of Urology*, Vol. 137, pp. 772–776, 1987.

24. Kilic, M., E. C. Serefoglu, A. T. Ozdemir and M. D. Balbay, "The Actual Incidence of Papaverine-Induced Priapism in Patients with Erectile Dysfunction Following Penile Colour Doppler Ultrasonography", *Andrologia*, Vol. 42, No. 1, pp. 1–4, 2010.

25. Kokalari, I., T. Karaja and M. Guerrisi, "Review on Lumped Parameter Method for Modeling the Blood Flow in Systemic Arteries", *Journal of Biomedical Science and Engineering*, Vol. 6, pp. 92–99, 2013.

26. Westerhof, N., F. Bosman, C. J. De Vries and A. Noordergraaf, "Analog Studies of the Human Systemic Arterial Tree", *Journal of Biomechanics*, Vol. 2, pp. 121–143, 1969.

27. Snyder, M. F., V. C. Rideout and R. J. Hillestad, "Computer Modeling of the Human Systemic Arterial Tree", *Journal of Biomechanics*, Vol. 1, pp. 341–353, 1968.

28. Sagawa, K., R. K. Lie and J. Schaefer, "Translation of Otto frank's paper "Die Grundform des Arteriellen Pulses" Zeitschrift fur Biologie 37: 483-526 (1899)",

Journal of Molecular and Cellulal Cardiology, Vol. 22, pp. 253–254, 1990.

29. Westerhof, N., J.-W. Lankhaar and B. E. Westerhof, "The Arterial Windkessel", *Medical & Biological Engineering & Computing*, Vol. 47, pp. 131–141, 2009.

30. Hoskins, P. R., P. V. Lawford and B. J. Doyle, *Cardiovascular Biomechanics*, Springer, Switzerland, 2017.

31. Patel, D. J., W. G. Austen, J. C. Greenfield and G. T. Tindall, "Impedance of Certain Large Blood Vessels in Man", *Annals of the New York Academy of Sciences*, Vol. 115, pp. 1129–1139, 1964.

32. Burattini, R. and S. Natalucci, "Complex and Frequency-Dependent Compliance of Viscoelastic Windkessel Resolves Contradictions in Elastic Windkessels", *Medical Engineering & Physics*, Vol. 20, No. 7, pp. 502–514, 1998.

33. Stergiopulos, N., B. E. Westerhof and N. Westerhof, "Total Arterial Inertance as the Fourth Element of the Windkessel Model", *The American Journal of Physiology*, Vol. 276, No. 1, pp. H81–H88, 1999.

34. Milišic, V. and A. Quarteroni, "Analysis of Lumped Parameter Models for Blood Flow Simulations and Their Relation with 1D Models", *ESAIM: Mathematical Modelling and Numerical Analysis*, Vol. 38, No. 4, pp. 613–632, 2004.

35. Spessoto, L. C. F., J. A. Cordeiro and J. M. P. De Godoy, "Effect of Systemic Arterial Pressure on Erectile Dysfunction in the Initial Stages of Chronic Arterial Insufficiency", *British Journal of Urology International*, Vol. 106, No. 11, pp. 1723–1725, 2010.

36. Padmanabhan, P. and A. R. Mccullough, "Penile Oxygen Saturation in the Flaccid and Erect Penis in Men with and without Erectile Dysfunction", *Journal of Andrology*, Vol. 28, No. 2, pp. 223–228, 2006.

37. Barnea, O., "A Theoretical Unidirectional Valve Based on Functional Collapse of Blood Vessels in the Penis", *Annals of Biomedical Engineering*, Vol. 25, pp. 470–476, 1997.

38. Borowitz, E. and O. Barnea, "Hemodynamic Mechanisms of Penile Erection", *IEEE Transactions on Biomedical Engineering*, Vol. 47, No. 3, pp. 319–326, 2000.

39. Gillon, G. and O. Barnea, "Erection Mechanism of the Penis: A Model Based Analysis", *Journal of Urology*, Vol. 168, pp. 2711–1715, 2002.

40. Barnea, O. and G. Gillon, "Cavernosometry: A Theoretical Analysis", *International Journal of Impotence Research*, Vol. 16, pp. 154–159, 2004.

41. Barnea, O., S. Hayun and G. Gillon, "A Mathematical Model of Penile Vascular Dysfunction and Its Application to a New Diagnostic Technique", *Annals of New York Academy of Sciences*, Vol. 1101, pp. 439–452, 2007.

42. Souper, R., J. Hartmann, M. Alvarez, I. Fuentes, G. Astroza and M. Marconi, "Correlation Between Peak Systolic Velocity and Diameter of Cavernosal Arteries in Flaccid Versus Dynamic State for the Evaluation of Erectile Dysfunction", *International Journal of Impotence Research*, Vol. 29, No. 4, pp. 132–135, 2017.

43. Chen, J., A. Gefen, A. Greenstein, H. Matzkin and D. Elad, "Predicting Penile Size During Erection", *International Journal of Impotence Research*, Vol. 12, pp. 328–33, 2000.

44. Ng, W. K., E. Y. K. Ng and S. J. Chia, "The Engineering Analysis of Bioheat Equation and Penile Hemodynamic Relationships in the Diagnosis of Erectile Dysfunction: Part I - Theoretical Study and Mathematical Modeling", *International Journal of Impotence Research*, Vol. 20, pp. 295–306, 2008.

45. Udelson, D., A. Nehra, D. G. Hatzichristou, K. Azadzoi, R. B. Moreland, J. Krane, I. Saenz de Tejada and I. Goldstein, "Engineering Analysis of Penile Hemodynamic

and Structural-Dynamic Relationships: Part II - Clinical Implications of Penile Tissue Mechanical Properties", *International Journal of Impotence Research*, Vol. 10, pp. 25–35, 1998.

46. Udelson, D., A. Nehra, D. G. Hatzichristou, K. Azadzoi, R. B. Moreland, J. Krane, I. Saenz de Tejada and I. Goldstein, "Engineering Analysis of Penile Hemodynamic and Structural-Dynamic Relationships: Part I - Clinical Implications of Penile Tissue Mechanical Properties", *International Journal of Impotence Research*, Vol. 10, pp. 15–24, 1998.

47. Sundareswaran, K. S., K. Pekkan, L. P. Dasi, K. Whitehead, S. Sharma, K. R. Kanter, M. A. Fogel and A. P. Yoganathan, "The Total Cavopulmonary Connection Resistance: A Significant Impact on Single Ventricle Hemodynamics at Rest and Exercise", Vol. 295, pp. H2427–H2435, 2008.

48. Yigit, M. B., W. J. Kowalski, D. J. R. Hutchon and K. Pekkan, "Transition from Fetal to Neonatal Circulation: Modeling the Effect of Umbilical Cord Clamping", *Journal of Biomechanics*, Vol. 48, No. 9, pp. 1662–1670, 2015.

49. Peskin, C. S. and C. Tu, "Hemodynamics in Congenital Heart Disease", *Computers in Biology and Medicine*, Vol. 16, No. 5, pp. 331–359, 1986.

50. Pekkan, K., D. Frakes, D. De Zelicourt, C. W. Lucas, W. J. Parks and A. P. Yoganathan, "Coupling Pediatric Ventricle Assist Devices to the Fontan Circulation: Simulations with a Lumped-Parameter Model", *ASAIO Journal*, Vol. 51, No. 5, pp. 618–628, 2005.

51. Wagner, G. and I. Saenz de Tejada, "Update on Male Erectile Dysfunction", *British Medical Journal*, Vol. 316, No. 7132, pp. 678–682, 1998.

52. Chen, K. K., Y. H. Chou, L. S. Chang and M. T. Chen, "Sonographic Measurement of Penile Erectile Volume", *Journal of Clinical Ultrasound*, Vol. 20, No. 4, pp. 247–

253, 1992.

53. McVeigh, G. E., A. Bank and J. N. Cohn, "Arterial Compliance", J. T. Willerson, H. J. J. Wellens, J. N. Cohn and D. R. Holmes Jr. (Editors), *Cardiovascular Medicine*, chap. 85, pp. 1811–1831, Springer, 3 edn, 2007.

54. Goktas, S., O. Yalcin, E. Ermek, S. Piskin, C. T. Capraz, Y. O. Cakmak and K. Pekkan, "Haemodynamic Recovery Properties of the Torsioned Testicular Artery Lumen", *Scientific Reports*, Vol. 7, No. 15570, pp. 1–9, 2017.

55. Kennedy, J. and R. Eberhart, "Particle Swarm Optimization", *Proceedings of the IEEE International Conference on Neural Networks*, Vol. 4, pp. 1942–1948, 1995.

56. Eberhart, R. and J. Kennedy, "A New Optimizer Using Particle Swarm Theory", pp. 39–43, 1995.

57. Eberhart, R. and Y. Shi, "Particle Swarm Optimization: Developments, Applications and Resources", *Proceedings of the 2001 Congress on Evolutionary Computation*, pp. 81–86, 2002.

58. Jegier, W., P. Sekelj, P. A. M. Auld, R. Simpson and M. McGregor, "The Relation Between Cardiac Output and Body Size", *British Heart Journal*, Vol. 25, pp. 425–430, 1963.

59. Du Bois, D. A. and E. F. Du Bois, "A Formula to Estimate the Approximate Surface Area if Height and Weight be Known", *The Archives of Internal Medicine*, Vol. 17, pp. 863–871, 1961.

60. Nelson, R. P. and T. F. Lue, "Determination of Erectile Penile Volume by Ultrasonography", *Journal of Urology*, Vol. 141, No. 5, pp. 1123–1126, 1989.

61. Lue, T. F., T. Takamura, R. A. Schmidt, A. J. Palubinskas and E. A. Tanagho, "Hemodynamics of Erection in the Monkey", *Journal of Urology*, Vol. 130, pp.

1237–1241, 1983.

62. Andersson, K.-E. and G. Wagner, "Physiology of Penile Erection", *Physiological Reviews*, Vol. 75, 1995.

APPENDIX A: CLINICAL MEASUREMENTS

Table A.1. All pre- and post-injection phase measurements for *Patient 1*. D and A represent the diameter and cross sectional area of cavernosal arteries and corpus cavernosum respectively, while *right* and *left* indices indicate the relevant side of penis

Parameter	**Patient 1**	
$P_{sa(systol)}/P_{sa(diastol)}$ *(mmHg)*	136 / 81	
CO (lt/min)	7.6	
	Pre-Injection Phase	**Post-Injection Phase**
$D_{cav,right}$ *(mm)*	0.7	1.1
$(PSV/EDV)_{right}$ *(dm/s)*	2.4 / 0	6.1 / -1.2
$A_{corp,right}$ (mm^2)	103.4	390.7
$D_{cav,left}$ *(mm)*	0.7	1.1
$(PSV/EDV)_{left}$ *(dm/s)*	2 / 0	5.6 / 0.9
$A_{corp,left}$ (mm^2)	103.7	387.7
ICP (mmHg)	**11.05**	**64.4**

Table A.2. All pre- and post-injection phase measurements for *Patient 2*, *Patient 3* and *Patient 4*. *D* and *A* represent the diameter and cross sectional area of cavernosal arteries and corpus cavernosum respectively, while *right* and *left* indices indicate the relevant side of penis

Variable	**Patient 2**	**Patient 3**	**Patient 4**
$P_{sa(systol)}/P_{sa(diastol)}$ *(mmHg)*	132 / 74	131 / 77	131 / 80
CO (lt/min)	6.36	6.8	6.06
Pre-Injection Phase			
$D_{cav,right}$ *(mm)*	0.5	0.5	0.8
$(PSV/EDV)_{right}$ *(dm/sn)*	2 / 0	2.3 / 0	1.8 / 0
$D_{cav,left}$ *(mm)*	0.5	0.5	0.8
$(PSV/EDV)_{left}$ *(dm/sn)*	2.2 / 0	2 / 0	1.6 / 0
ICP (mmHg)	**11.8**	**9.5**	**12.02**
Post-Injection Phase			
$D_{cav,right}$ *(mm)*	1.2	1.1	1.1
$(PSV/EDV)_{right}$ *(dm/sn)*	3.8 / 0	5.1 / -1.2	Not applicable
$D_{cav,left}$ *(mm)*	1.3	1.2	1
$(PSV/EDV)_{left}$ *(dm/sn)*	4 / 0	5.1 / -1.2	Not applicable
ICP (mmHg)	**65.2**	**52**	**Not applicable**

APPENDIX B: COMPLIANCE AND RESISTANCE VALUES OF THE LPM PARAMETERS

Table B.1. Main circulation values for the normal resting man [9]

Ideal Person	
$P_{sa(systol)}/P_{sa(diastol)}$ *(mmHg)*	120 / 80
CO (lt/min)	5.6
R_{sys} *(WU)*	17.5
C_{sa} *(lt/mmHg)*	0.01
C_{sv} *(lt/mmHg)*	1.75

Table B.2. Lower (LB) and upper bounds (UB) of the optimum point searching region for compliances and resistances in pre-injection phase of erection

Pre-Injection Phase										
Parameter	C_{sa}	C_{sv}	R_{sys}	C_{cav}	C_{corp}	C_{ven}	R_{hel}	R_{cav}	$R_{pv,out}$	R_{out}
LB	9e-4	0.1	10	1e-6	1e-4	1e-5	5000	10000	100	1000
UB	0.01	2	20	9e-6	1e-3	9e-5	15000	20000	1000	5000

Table B.3. Lower (LB) and upper bounds (UB) of the optimum point searching region for compliance and resistances in post-injection phase of erection

Post-Injection Phase										
Parameter	C_{sa}	C_{sv}	R_{sys}	C_{cav}	C_{corp}	C_{ven}	R_{hel}	R_{cav}	$R_{pv,out}$	R_{out}
LB	9e-4	0.1	10	1e-6	1e-4	1e-5	100	1000	100	1000
UB	0.01	2	20	9e-6	9e-4	9e-5	1000	5000	3000	5000

Table B.4. The determined resistance (WU) and compliance (lt/mmHg) values for each patient and phase of erection

Parameter	**Patient 1**		**Patient 2**		**Patient 3**		**Patient 4**	
	Pre-Injection	**Post-Injection**	**Pre-Injection**	**Post-Injection**	**Pre-Injection**	**Post-Injection**	**Pre-Injection**	**Post-Injection**
C_{sa}	0.0013	0.0013	9.78e-4	9.28e-4	0.0011	0.0011	9.75e-4	Not applicable
C_{sv}	0.42	0.38	1.04	1.37	0.73	0.71	1.07	Not applicable
R_{sys}	14.04	14.02	16.20	16.95	15.19	15.20	16.11	Not applicable
C_{cav}	1e-6	2.4e-6	1e-6	1e-6	9e-6	5.32e-6	9e-6	Not applicable
C_{corp}	0.0012	9.34e-4	8.77e-4	4.95e-4	3.92e-4	3.47e-4	1e-4	Not calculated
C_{ven}	1.02e-5	2.19e-5	5.42e-5	1.62e-5	9e-5	1e-5	4.35e-5	Not applicable
R_{hel}	4840	500	15000	263	12633	553	15591	Not applicable
R_{cav}	15147	1656	18439	2067	16559	4418	16698	Not applicable
$R_{pv,out}$	1891	1750	601	50	118	2713	1835	Not applicable
R_{out}	181	1130	2662	3308	1933	1806	500	Not applicable